

**FLEXURAL STRENGTH INVESTIGATION ON  
COLD-FORMED STEEL FACE-TO-FACE  
C-SECTION BEAM**

**BY**

**HA THANH TRAN**

**A THESIS SUBMITTED IN PARTIAL FULFILLMENT OF THE  
REQUIREMENTS FOR THE DEGREE OF MASTER OF SCIENCE  
(ENGINEERING AND TECHNOLOGY)**

**SIRINDHORN INTERNATIONAL INSTITUTE OF TECHNOLOGY**

**THAMMASAT UNIVERSITY**

**ACADEMIC YEAR 2015**

**FLEXURAL STRENGTH INVESTIGATION ON  
COLD-FORMED STEEL FACE-TO-FACE  
C-SECTION BEAM**

**BY**

**HA THANH TRAN**

**A THESIS SUBMITTED IN PARTIAL FULFILLMENT OF THE  
REQUIREMENTS FOR THE DEGREE OF MASTER OF SCIENCE  
(ENGINEERING AND TECHNOLOGY)**

**SIRINDHORN INTERNATIONAL INSTITUTE OF TECH**

**THAMMASAT UNIVERSITY**

**ACADEMIC YEAR 2015**



FLEXURAL STRENGTH INVESTIGATION ON COLD-FORMED STEEL  
FACE-TO-FACE C-SECTION BEAM

A Thesis Presented

By

HA THANH TRAN

Submitted to

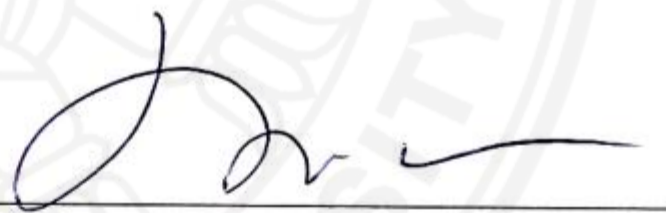
Sirindhorn International Institute of Technology

Thammasat University

In partial fulfillment of the requirements for the degree of  
MASTER OF SCIENCE (ENGINEERING AND TECHNOLOGY)

Approved as to style and content by

Advisor and Chairperson of Thesis Committee



(Assoc. Prof. Dr. Taweep Chaisomphob)

Committee Member and  
Chairperson of Examination Committee



(Prof. Dr. Pruettha Nanakorn)

Committee Member



(Assoc. Prof. Dr. Trakool Aramraks)

DECEMBER 2015

## Abstract

### FLEXURAL STRENGTH INVESTIGATION ON COLD-FORMED STEEL FACE-TO-FACE C SECTION BEAM

By

HA THANH TRAN

Degree Bachelor, Ho Chi Minh City University of Technology, VietNam, 2011

Cold-formed steel C-section beams are mostly used in the construction industry. In cold-formed steel constructions, built-up beams are often assembled from two single C-sections such as face-to-face C-section so as to achieve a structurally desirable cold-formed steel section. However, the buckling behaviour of face-to-face C-section beams have not been investigated yet in the literature. Furthermore, the current design code such as AISI-2012 does not provide any guideline on this issue. Therefore, this research was conducted by experimental and numerical analyses in order to investigate the flexural behaviour of face-to-face C-section beam affected by different connection spacing. The built-up sections studied in this research were made from two C-section with their both flanges placed face-to-face which is connected by using stiffening plates and four self-drilling screws at varied connection spacing. Firstly, a total of twelve cases of three different dimension of C-section and four varied connection spacing for each beam were tested to evaluate the main failure modes and the ultimate moment capacity of the beams. Based on the popular use in Thailand, three sizes of C-section C15019, C15024 and C20019 were selected to assemble three series of built-up beams. The test specimens C15019 was named as follows: C150 denotes the C-channel section with 150mm web depth, the final number of 19 denotes the thickness of 1.9mm and the clear span (L) was 3.6m. The test results showed that for the C15019 beam, the maximum load and failure mode are the same for the case of L/6 and L/4. Similar conclusion was also drawn for the C20019 beam, the maximum load and failure mode are the same for the case of L/6 and L/4. For the C15024 beam, the maximum

load and failure mode are the same for the case of L/6, L/4 and L/3. This means that limit connection spacing of L/6 stipulated in AISI-2012 may be unconservative. After that, a comparison between the test results and Specification AISI (2012 ed.) was then performed. The comparison proves that the Specification was conservative for the face-to-face C-section beam that was governed by local buckling at failure mode. Finally, a nonlinear finite element analysis including the effects of material nonlinearities, initial geometric imperfections was performed to simulate the test beam. The results from numerical analyses were compared with the test results to validate the model. Good agreement was obtained between experimental and numerical results, proving the validity of the proposed FEM in this study.

**Keywords:** Cold-formed steel beam, Flexural behavior, Built-up C section.

## **Acknowledgements**

Primarily, I would like to express my deepest gratitude to my advisor Assoc. Prof. Taweep Chaisomphob for the guidance in my research of master program. In all two academic years, I have studied a lot from him and I appreciate all his contributions of time, ideas, and funding for my study.

I would like to acknowledge my dissertation committee members Prof. Pruettha Nanakorn and Assoc. Prof. Trakool Aramraks, who gave me valuable comments on my thesis to make it better. I would also like to acknowledge Prof. Eiki Yamaguchi, Kyushu Institute of Technology, Japan for his suggestion on the part of discussion on the test and numerical results.

Finally, I would like to acknowledge Sirindhorn International Institute of Technology, Thammasat University for their scholarship. I also thank the School of Civil Engineering for their support and assistance during my master program and BlueScope Lysaght (Thailand) Limited Company for their financial support.

## Table of Contents

Chapter	Title	Page
	Signature Page	i
	Abstract	ii
	Acknowledgements	iv
	Table of Contents	v
	List of Tables	vii
	List of Figures	viii
1	Introduction	1
	1.1. General	1
	1.2. Current Type of Cold-formed Steel in ThaiLand	4
	1.3. Research problem	5
	1.4. Objectives	7
	1.5. Scope of study	7
2	Literature Review	9
	2.1. General	9
	2.2. Cold-formed Steel Design Specification	9
	2.3. Past experimental and numerical studies	13
	2.4. Type of connection	17
3	Experimental Investigation	19
	3.1. Test specimen	19
	3.2. Test set-up	21
	3.3. Test procedure	23
	3.4. Material properties	25
	3.5. Test results	26
4	Numerical Investigation	32
	4.1. Introduction	32
	4.2. Finite element and mesh	33

4.3. Material modelling	34
4.4. Loading, boundary and contact condition	34
4.5. Finite element analysis	37
4.6. Comparison between numerical and test results	37
4.6.1 Load–vertical displacement comparison	37
4.6.2 Main failure mode	39
5 Conclusions and recommendation	41
References	42



## List of Tables

Tables	Page
1.1. Dimension C section in Thailand	5
3.1. Standard range of LYSAGHT Cees section	19
3.2. Dimension of C-section use in this research	20
3.3. Summary test result of the beam corresponding to CS variation	26
3.4. Comparison of moment capacity from test and design rule for built-up face-to-face beam	31
4.1 Comparison of FEM and test results	38

## List of Figures

Figures	Page
1.1. Various sections of cold-formed steel	1
1.2. Some applications of cold-formed steel	2
1.3. CFS producing step	3
1.4. Cee and Zee section	4
2.1. Buckling failure mode of CFS C-sections: (a): Local buckling; (b): lateral distortional buckling; (c): flange distortional buckling; (d): lateral-torsional buckling	10
2.2. Box beam edge loading	14
2.3. Built-up box section	15
2.4. Scheme of cross sections of the tested beam	17
2.5. Connectors used in CFS Construction	17
2.6. Screw connections in the test	18
3.1. C cross section	20
3.2. Face-to-face built-up C specimen (C15019)	21
3.3. Overall view of bending test	22
3.4. Support system: (a): Roller support; (b): Pinned support	22
3.5. Detail of measurements : (a): Strain gauge; (b): LVDT; (c) (d): data logger	23
3.6. (a) Schematic diagram of four-point bending test with CS of L/6; (b) Cross section M	24
3.7. Top and bottom view of connector arrangement with CS of L/6	24
3.8. (a): Dimension of tensile coupon specimen (b): Stress-strain curve for the specimens	25
3.9. (a): Load-displacement curve for F2F-C15019 with CS L/6 ; L/4; L/3; L/2	28
3.10: Load-displacement curve for F2F-C15024 with CS L/6 ; L/4; L/3; L/2	28
3.11 : Load-displacement curve for F2F-C20019 with CS L/6; L/4; L/3; L/2	29
3.12 : Load-strain for F2F-C15019 with connection spacing of L/6, L/4	29
3.13 : Load-strain for F2F-C15019 with connection spacing of L/3, L/2	29
4.1. FEM model for beam with connection spacing L/2	33
4.2. Mesh modelling	34

4.3. A simplified model for four-point bending test	35
4.4. (a) Loading modelling, (b) A simplified pinned,roller support conditions	35
4.5. Contact modelling between the rigid support and C section	36



# Chapter 1

## Introduction

### 1.1. General

Hot-rolled steel has been used in steel construction in the past long history and had many applications in the steel construction. Nevertheless, the new steel material produced by cold roll forming process from steel sheet or plate has been used significantly recently. The construction project of the large housing village is widely used cold-formed steel technology in Thailand. Thin gauges of sheet steel was roll-formed or pressed to make the common term for products, namely cold-formed steel (CFS). Some CFS sections was popularly used in structural design building shown in Figure 1.1. Some types of product made from CFS were introduced into construction market such as ducting, gutter, roofing, walling, shutters, roller doors, framing, trusses, louvers, ceiling, partition, and so on.



Figure 1.1. Various sections of cold-formed steel

CFS has become an increasingly integral part of the construction and building industries since the middle of the 20th century when design procedures and standard were established to cater for its use. Thin gauges of sheet steel was used to create thin-walled structural elements and non-structural elements in the construction

industry such as beams, columns, floor decking, studs, joists, built-up sections and other components. In building construction, C-section with lips or without lips and Z sections are most popular used as cold-formed steel structure. Steel structure used CFS material as main structure was commonly applied from commercial buildings to larger industrial and residential housing. CFS beam can be used as floor joists and bearers, wall studs, roof purlins and rafters. There are some construction structures used CFS as the main material such as bridges, buildings, storage racks, car bodies, grain bins, various types of equipment, transmission towers, railway, highway products, drainage facilities, transmission poles and others (Figure 1.2).



Figure 1.2. Some applications of cold-formed steel

There are three methods to make the section of CFS: bending brake operation, press brake operation and cold roll forming. Cold roll forming method was popularly used in the manufacturing of CFS sections by using steel sheet, flat bar, plate or strip which are cold-formed in roll forming machines. There is quite different in the manufacturing between CFS products and traditional hot-rolled steel products which is produced at room temperature using pressing or rolling (Figure 1.3) for CFS products. The strength to weight ratio of CFS section members is higher than that of hot-rolled steel since CFS section was increased yield strength from the initial steel sheet strength that was produced during the cold roll forming method which may cause the strain hardening to CFS sections. Some angles, Z or channel sections were produced by press brake operation. In general, there are large variations of the

material thicknesses for CFS section which usually range from 0.373 mm to 6.35 mm. For steel sheet, the thickness often varies from 0.3 mm to 4 mm which are usually used for non-structural applications such as floor decking or steel panels. But for some structural applications which carry a heavy load such as beams or columns, the thickness of sections varies from 1.2 mm to 6.4 mm.



Figure 1.3. CFS producing step

Generally, cold-formed steels (CFS) structure are easily for installation because of its lightweight and high durability. Some advantages of CFS can be realized when compared with other traditional materials (concrete, timber) as following: lightness, easy and fast erection, easy and fast installation, ease of prefabrication, high strength and stiffness, noncombustibility, more accurate detailing, formwork unneeded, noncreeping and nonshrinking at ambient temperatures, recyclable material, economy in handling.

Buckling is the predominant failure mode in CFS steel structure, so it should be considered carefully in CFS design. Screws were commonly used to assemble stud frames in the CFS steel structure, which are similar to timber structure. In some area, the big beam sizes are needed to resist the large load and moment. There are limited sizes of material due to the distance of the construction and difficultly to order variety of sections. To increase capacity of the single section, the built-up section are commonly used.

## 1.2. Current Type of Cold-formed Steel in Thailand

Some types of CFS such as C-section and Z sections are mostly used in building construction in Thailand. Applications of CFS are numerous ranging from residential housing to larger industrial and commercial buildings. CFS can be used as floor joists and bearers, wall studs, and roof purlins and rafters. In cold-formed steel constructions in Thailand, built-up beams are often assembled from two single C sections. Assembling two C sections together is a technique which can achieve a structurally desirable cold-formed steel section. With this technique, the structural bending capacity of the beam is expected to be more capacity than single section. Traditional, face-to-face C-sections or nested C-sections forming a box girder are the most popular built-up section in the construction industry Thailand.

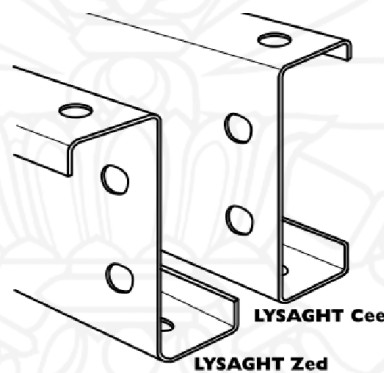
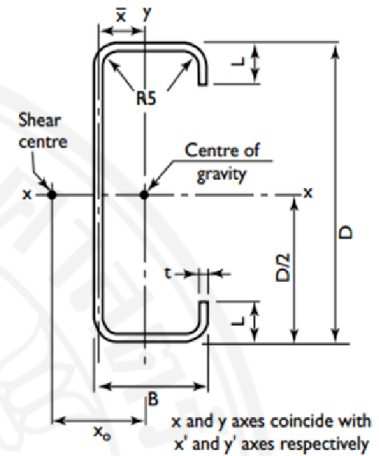


Figure 1.4. Cee and Zee section

Currently there are 16 variations of the C section which range from a depth of 102 mm to 350 mm while the width of the C section varies from 51 mm to 125 mm and the thickness of CFS used for the beams varies from 1.0 mm to 3.0 mm that are available in Thailand. Because of limitations of transportation, the available length of CFS products is limited such as 6, 8, 10m. Table 1.1 shows the section dimensions for the range of commercially available C sections.

Table 1.1. Dimension C section in Thailand

Catalogue Number	t mm	D mm	B mm	L mm	Mass per unit length(kg/m)
C10010	1.0	102	51	12.5	1.78
C10012	1.2	102	51	12.5	2.10
C10015	1.5	102	51	13.5	2.62
C10019	1.9	102	51	14.5	3.29
C15012	1.2	152	64	14.5	2.89
C15015	1.5	152	64	15.5	3.59
C15019	1.9	152	64	16.5	4.51
C15024	2.4	152	64	18.5	5.70
C20015	1.5	203	76	15.5	4.49
C20019	1.9	203	76	19.0	5.74
C20024	2.4	203	76	21.0	7.24
C25019	1.9	254	76	18.5	6.50
C25024	2.4	254	76	20.5	8.16
C30024	2.4	300	96	27.5	10.09
C30030	3.0	300	96	31.5	12.76
C35030	3.0	350	125	30.0	15.23



### 1.3. Research problem

Some types of cold-formed steel such as C-section with lips or without lips, and Z sections are normally used as flexural members in Thailand. The built-up beam made of face-to-face C-sections are normally used as flexural combination members so as to improve the flexural capacity of section, when single C sections are not sufficient for bearing loads.

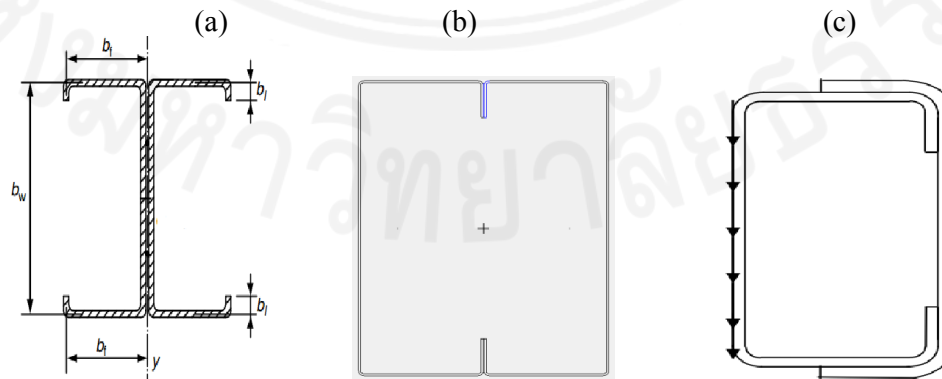


Figure 1.5. (a) Back-to-back; (b) face-to-face C-sections ; (c) nested C-sections



The increasing use of CFS built-up section in the construction industry is a direct result of continuing research into the more complicated behaviour of these sections, and their superior cross section geometry that is facilitated by improved cold-formed manufacturing processes, high yield strength base steels, and innovative cross section geometries. However, the flexural behaviour of face-to-face C-section including their buckling characteristics has not been investigated yet. Furthermore, there are no specific guideline for face-to-face C-section such as the current design code North American Specification (AISI 2012), Australian/New Zealand Standard (AS/NZS 2005) and European Code (EN1993). The AISI is limited to built-up I sections and suggested that the moment capacity and moment of inertia of those compound beams are the simple addition of the component parts. This assumption was made based on the assumption of displacement compatibility among the component parts but has not been confirmed by testing. Therefore, for this study, a face-to-face built-up C-sections shown in (Figure 1.6) need to be investigated to study the structural strength of CFS face-to-face C beam under uniform bending moment and to provide clear design guidance. This will be useful for designer and other practicing engineers.

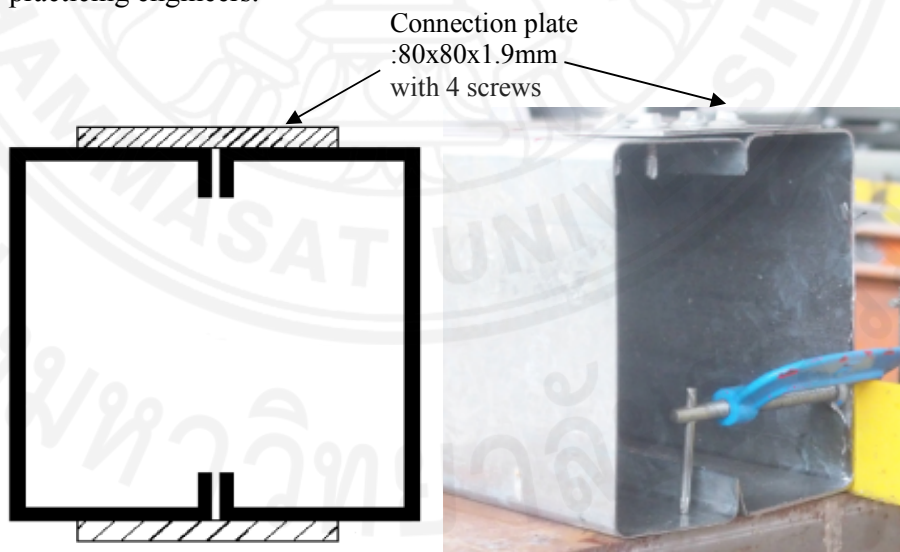


Figure 1.6. Face-to-face built-up C-sections

In this research, screws connection are made to connected two C-sections because screw is a common type of connections that is used in CFS to connect each individual part together. Screw connection provides advantages in fast installation and simple design. By using additional stiff plate with 4 screws, the built-up section is connected together instead of welding because of its thin thickness and can be increased the bending capacity of the beam to some extent.

#### **1.4. Objectives**

The objective of this study is to study the flexural behaviour of cold-formed steel face-to-face built-up C-sections affected by different connection spacing and to verify whether the face-to-face built-up C-sections CFS can be designed using the current design equations specified in North American Specification AISI (2012 ed.), namely Direct Strength Method (DSM).

The main objectives of this study can be summarized as:

- ✚ Experimental study: Four-point bending tests were conducted.
- ✚ Numerical study: A finite element model was developed using ABAQUS (version 6.12) and a comparison between the experimental results and numerical model was then performed.
- ✚ Design rules standard: assess and compare the beam strength of intermittently connection spacing face-to-face C-section beam in this research against the continuous connection spacing of those beams according to current design codes.

#### **1.5. Scope of study**

- ✚ The face-to-face C-section beams studied in this research were made from two C-sections with their both flanges placed face-to-face which is connected by using stiff plates that were fastened with 4 self-drilling screws at varied connection spacing.
- ✚ The experimental C-section has been limited because of limitations of commercially available C-section cold-formed steel in Thailand market.
- ✚ Conduct a series of face-to-face C-section beams subject to four-point bending test for intermediate span length, namely 4m.

✚ The CFS C-section used in this study had 485 MPa yield strength ( $F_y$ ) and 528 MPa ultimate strength ( $F_u$ ).



## **Chapter 2**

### **Literature Review**

#### **2.1. General**

With the aim of providing some background knowledge related to flexural behaviour of the CFS built-up section, the current design practice, experimental and numerical studies in the past were reviewed. Firstly, a brief review of design specification of CFS structural members was provided. After that, previous researches in this field including all experimental and numerical studies of built-up C section were also discussed briefly.

#### **2.2. Cold-formed Steel Design Specification**

Some types of CFS such as C-section with lips or without lips, and Z-sections can be used as flexural members in Thailand. To improve the flexural capacity of section, some types of built-up sections such as back-to-back C-sections, nested C-sections forming a box girder or face-to-face C-sections are normally used as flexural combination members when single C sections are not sufficient for bearing loads. In some CFS flexural members design codes, lateral buckling of the beam was governed by the flexural behavior of the member, especially when built-up sections made of thin individual section and insufficiently lateral restraint. This buckling of CFS consists of either lateral-torsional buckling, local buckling, lateral distortional buckling or interactive buckling mode depending on the location of loading, the geometry and lateral support given (Figure 2.1). Because of the thin material used, the CFS flexural section is also more prone to fail by distortional or local buckling in contrast to hot-rolled steel. Therefore, the bracing requirements should be provided adequately for flexural members in accordance with the current design code North American Specification (AISI 2012).

The current design code AISI 2012 provides two design approach to calculate flexural strength moment capacity of single members. Firstly, in approach I, the

assumption of “initiation of yielding” is provided. After that, the assumption of “inelastic reserve capacity” is provided lately in approach II.

In approach I: AISI 2012 stipulated that the nominal moment capacity ( $M_n$ ) of CFS section was defined as the effective yielding moment ( $M_y$ ) calculated depends on the flange and web effective areas of the section. The effective yielding moment  $M_y$  is suggested on the basis of the moment at which the outer fiber first attains yields. For a balanced section, the stress in tension and compression at the outer fibres achieves the yield strength simultaneously. But for an eccentrically located neutral axis, initiation of yielding can take place either in the compression flange or tension flange. The nominal moment capacity ( $M_n$ ) is the same as the effective yielding moment ( $M_y$ ) and can be calculated by using the following equation:

$$M_n = M_y = S_e F_y \quad (2.1)$$

Where  $F_y$ : material’s yield strength, and  $S_e$ : the effective elastic section modulus of the full section and can be calculated by considering the effective width of individual elements of the beam under design yield stress  $F_y$ .

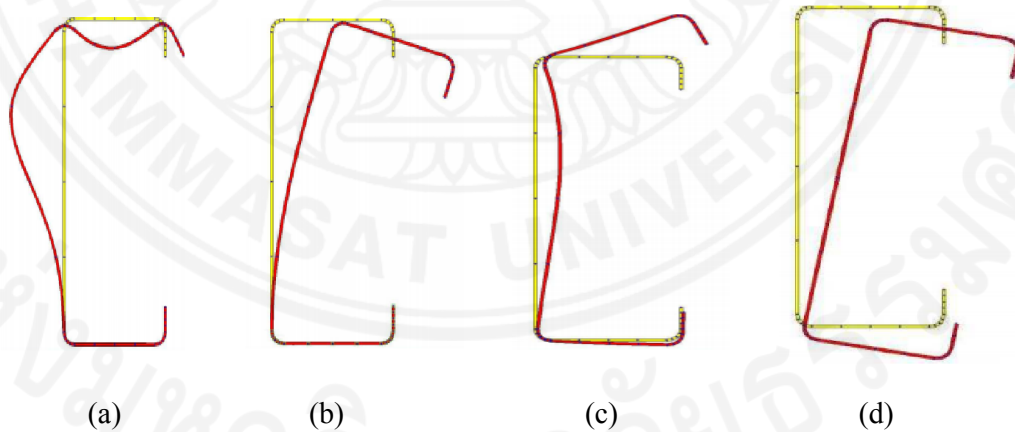


Figure 2.1. Buckling failure mode of CFS C-sections: (a): Local buckling; (b): lateral distortional buckling; (c): flange distortional buckling; (d): lateral-torsional buckling

In approach II: due to the high width-to-thickness ratios of CFS elements which is usually excessive the plastic design limitation, the AISI Specification has not provided the inelastic reserve capacity of beams method before 1980. Because the

width-to-thickness ratios of the section is usually large, CFS members usually buckle before reaching plastic hinges such as local buckling. By considering the partial plastification process that develop through the full section, the inelastic reserve strength was considered to calculate the nominal moment  $M_n$ . In the compression flange, the maximum strain ( $\epsilon_{cu}$ ) was used to calculate the inelastic stress distribution.

Furthermore, there are no specific guideline for face-to-face C section such as the current design code North American Specification (AISI 2012), Australian/New Zealand Standard (AS/NZS 2005) and European Code (EN 1993). For the built-up flexural members such as I-sections that are often assembled from two single C sections by mean of welds or other connectors, the spacing of connectors is provided the limited guideline by AISI (2012 ed.). To ensure the full I-section behave as a single section and prevent failure of connectors, AISI stipulated that the maximum longitudinal spacing of connections should be the smaller value between  $L/6$  or  $2gT_s/mq$  (Equation D1.1-1) , where  $L$ = beam's span;  $g$  = vertical distance between two rows of connections;  $T_s$ = design strength of connection in tension;  $m$ = distance from shear center of one C-section to mid-plane of web;  $q$ = design load on beam. In addition, the limited spacing  $L/6$  is required to prevent any buckling on the top flange of the I-sections between connections. Nevertheless, there are no guideline for face-to-face C-section beam in the current design code such as AISI-2012.

Currently there are no available design equations specified in North American Specification AISI (2012 ed.) to calculate the beam strength of intermittently fastened face-to-face CFS built-up beam. AISI (2012 ed.) specifies a design rule for compound sections composed of two or more single section in a beam with continuous connection to predict the beam strength. Therefore, the current design rule is not suitable for intermittently fastened face-to-face CFS built-up beam. With the aim of evaluating the strength of tested beam, it is necessary to assess and compare the beam strength of intermittently fastened face-to-face CFS built-up beam in this research against the continuous connection of those beams according to current design codes.

According to Appendix 1 of the North American Specification AISI (2012 ed.), the design moment strength of the beam was calculated by using the Direct Strength Method (DSM). The nominal moment capacity ( $M_n$ ) is the lowest value of the lateral-torsional buckling strength ( $M_{ne}$ ), local buckling strength ( $M_{nl}$ ) and the distortional buckling strength ( $M_{nd}$ ) in accordance with Section 1.2.2.1.1, 1.2.2.1.2 and 1.2.2.1.3 of Appendix 1–AISI (2012 ed.), respectively.

The nominal moment capacity for lateral–torsional buckling strength ( $M_{ne}$ ) is calculated as follows:

$$\text{For } M_{cre} < 0.56M_y : \quad M_{ne} = M_{cre} \quad (2.2)$$

$$\text{For } 0.56M_y \leq M_{cre} \leq 2.78M_y: \quad M_{ne} = \frac{10}{9} M_y \left( 1 - \frac{10M_y}{36M_{cre}} \right) \quad (2.3)$$

$$\text{For } M_{cre} > 2.78M_y : \quad M_{ne} = M_y \quad (2.4)$$

Where  $M_{cre}$  is the critical elastic lateral–torsional buckling moment of the section:  $M_{cre} = f_{cre}S_f$ ,  $f_{cre}$  is the elastic lateral–torsional buckling stress of the section;  $S_f$  is elastic section modulus of the full section relative to extreme first yield fiber; and finally  $M_y$  is yield moment of the full section:  $M_y = F_y S_f$ .

The nominal moment capacity for local buckling strength ( $M_{nl}$ ) is calculated as follows:

$$\text{For } \lambda_\ell \leq 0.776 : \quad M_{nl} = M_{ne} \quad (2.5)$$

$$\text{For } \lambda_\ell > 0.776: \quad M_{nl} = \left( 1 - 0.15 \left( \frac{M_{cr\ell}}{M_{ne}} \right)^{0.4} \right) \left( \frac{M_{cr\ell}}{M_{ne}} \right)^{0.4} M_{ne} \quad (2.6)$$

Where  $\lambda_\ell$  is slenderness factor used to calculate  $M_{nl}$ :  $\lambda_\ell = \sqrt{M_{ne} / M_{cr\ell}}$ ;  $M_{cr\ell}$  is the critical elastic local buckling moment of the section:  $M_{cr\ell} = f_{cr\ell} S_f$ ,  $f_{cr\ell}$  is the elastic local buckling stress of the section.

The nominal moment capacity for distortional buckling strength ( $M_{nd}$ ) is calculated as follows:

$$\text{For } \lambda_d \leq 0.673 : \quad M_{nd} = M_y \quad (2.7)$$

$$\text{For } \lambda_d > 0.673 : M_{nd} = \left( 1 - 0.22 \left( \frac{M_{crd}}{M_y} \right)^{0.5} \right) \left( \frac{M_{crd}}{M_y} \right)^{0.5} M_y \quad (2.8)$$

Where  $\lambda_d$  is slenderness factor used to calculate  $M_{nd}$ :  $\lambda_d = \sqrt{M_y / M_{crd}}$ ;  $M_{crd}$  is the critical elastic distortional buckling moment of the section:  $M_{crd} = f_{crd} S_f$ ;  $f_{crd}$  is the elastic distortional buckling stress of the section.

### 2.3. Past experimental and numerical studies

Serrette (2004) conducted a research to investigate the flexural behaviour of rafter box beams subjected to eccentric loading using both experimental testing and numerical studies (Figure. 2.2). The box beam was made of two channels, facing each other, connected by top and bottom tracks. At the bearing supports, the extension of the top and bottom tracks was not performed. Three different types of box beams configuration, same in section depth and width and with thicknesses of 1.09, 1.37 and 1.73 mm to form a box, were evaluated for this test program. To connect the tracks and joists together, a self-drilling screws were used on the web of joists close to flanges at 304.8 mm spacings. The test results reported that the main cause of failure mode for the beams subjected to the eccentric loading is twist. After that, the analytically computed capacities of the beam using a commercial software program was conducted to compare with the test results. The analytically computed capacities based on the assumption that lateral buckling of the beam is restrained and there is no lateral movement between the box beam parts. This assumption, noncomposite behaviour, contradicts with the proposed research as the purpose of this research is to investigate the additional increment in flexural capacity when considering composite actions. The test results data suggested that the box beam's capacity can be reduced 10-15% due to the edge loading condition. This research was conducted to investigate the effects of load distribution within the components and edge loading, but it did not address any behaviour of composite actions.



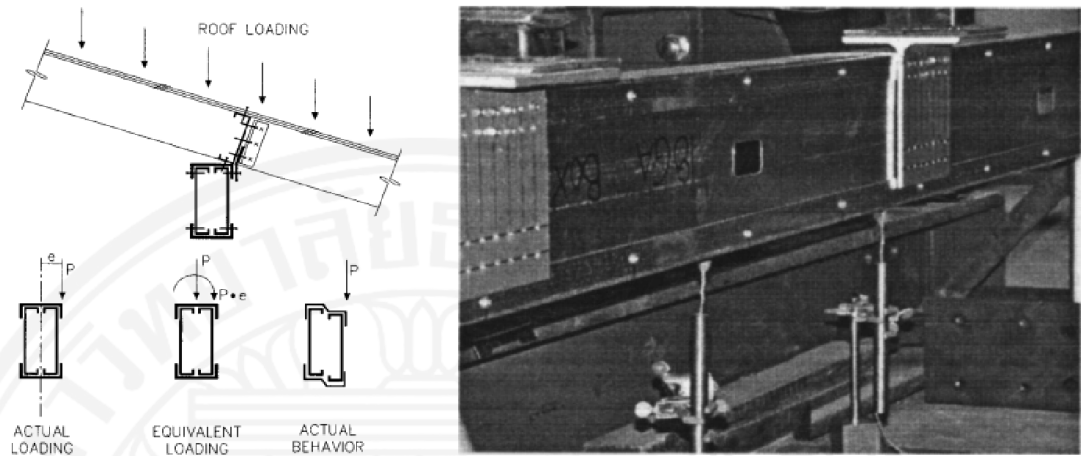


Figure 2.2. Box beam edge loading

Yu, C and Schafer (2006) did series of bending tests on CFS C and Z sections to deal with distortional buckling and local buckling phenomena. Iman (2015) studied the effect of top cover plates on cold-formed C-channels stiffened beam under moments and shear. The results was compared against the strength calculated by using Direct Strength Method (DSM) according to Appendix 1 of AISI (2012 ed.). Wang and Zhang (2009) carried out numerical and experimental study on the behaviour of various C-sections with different edge stiffeners subjected to four-point bending and non-four-point bending. The results show that the beam strength was greatly affected by the buckling mode and edge stiffener. Experimental investigation on high strength C and Z section subjected to bending was conducted by Pham and Hancock (2013). Two types of test with and without straps that was screwed on the top flanges of section to create local or distortional buckling was performed, respectively. The authors recommended formulas for calculating DSM strength design of nondimensional slenderness section based on the current formulas in codes. Nguyen (2006) studied the behavior of CFS Z-sections with complex and simple edge stiffener under axis bending by experimental and numerical investigations.

Lei Xu, et al (2009) presented in their research involving numerical analyses to study the bending capacity of built-up CFS box beam (Figure. 2.3). They developed the numerical model to study flexural behavior of CFS built-up box girder assembled from track section and C-shape by using screw connection. They stated about the moment capacity and moment of inertia of those compound beams are the simple addition of the component parts based on deflection compatibility of each component parts. In their study, the numerical model development was conducted to calculate the moment capacity of CFS built-up beam for concentric and eccentric loading and then compared with the tested results conducted by Beshara and Lawson (2003). Furthermore, from the adequate results in finite element model, more than 30 specimens with different section were carried out to study the affect of the height, thickness, applied load location (eccentric loading and concentric loading), screw spacing, steel yield strength on the bending behavior of CFS built-up box beam. As the results, the moment capacity of built-up CFS beam can be simple addition of the moment capacities of each component parts for concentric loading case. However, the above conclusion is inappropriate for eccentric loading case. A calibration coefficient of 0.9 is proposed to be used to calculate the moment capacity of the built-up CFS beam as the simple addition of the moment capacities of each component parts for eccentric loading case.

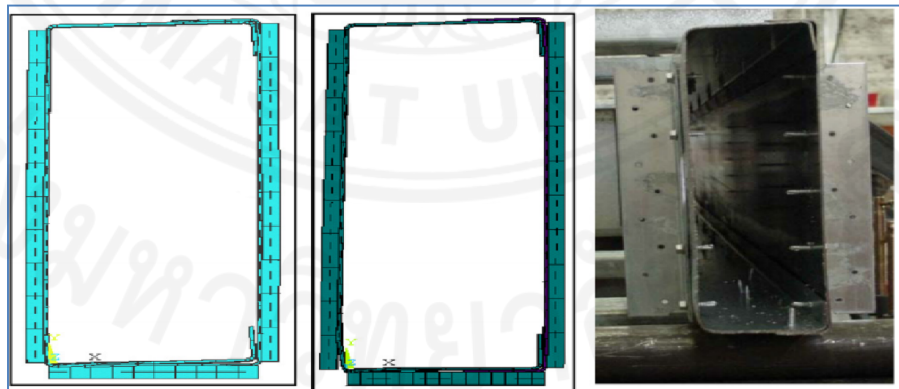


Figure 2.3. Built-up box section

Xu-hong Zhou and Yu Shi (2009) evaluated the flexural capacity of CFS built-up I-beams with lip-reinforced by experiment and finite element analysis. In the test, they investigated a total of 9 I-beams with three series and 3 identical specimens for each series. The series of experiment are conducted to obtain the flexural behaviour of the beam. After that, numerical analyses are undertaken to validate the experimental results. Results of experiment and finite element analysis results agree well, proving the validity of the finite element method. The effective compression flanges was greatly affected by the steel grade and flanges width-to-thickness ratio, while the length of the beam, the web height-to-thickness ratio, and the thickness of the plate have relatively little influence. Finally, based on results of parametric analyses, the author proposed the strength-reduction method and effective width method on ultimate moment capacity of cold-formed I-beams. Moreover, tables and equations, which are used to determine strength-reduction factors of built-up I-beams with typical sections, are gained. The ultimate load-carrying capacity from these methods agrees well with experimental results.

Laím et al. (2013) conducted 12 quasi-static bending tests at ambient temperature so as to evaluate the failure modes and moment capacity of CFS beams. They carried out four types of beams assembled from U and C single sections, namely C; I; R and 2R beam. For each beam, 3 identical tests were conducted in order to make a comparison (Figure 2.4). All sections with the same thickness of 2.5 mm, inside corner radius of 2 mm, and nominal flange width of 43 mm were used in the tests. After that, the numerical analyses were undertaken to compare with the experimental result. The test result proven the good agreement between the numerical and experimental. The failure buckling modes shown in the numerical analysis are also consistent with that of the tests. Further more, so as to evaluate the effect of height, thickness, and length of the beam to the moment capacity of the beam, fifty-two finite element models were undertaken. They concluded that when span length increases, especially, from 3.0 to 4, the strength of the beams decreases a lot.

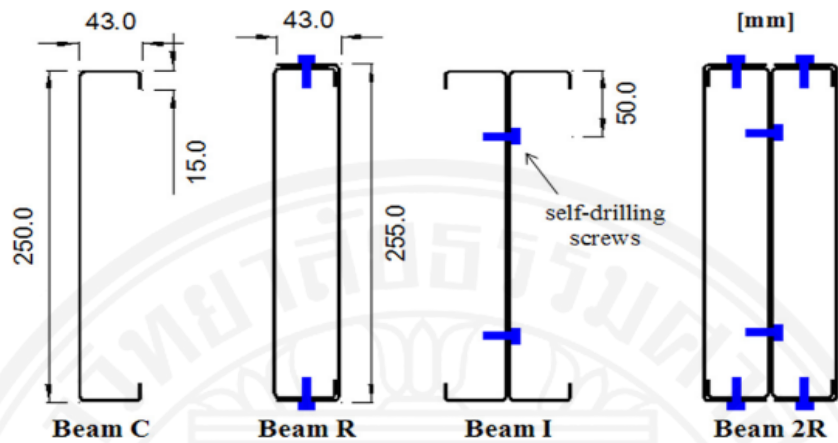


Figure 2.4. Scheme of cross sections of the tested beam

#### 2.4. Type of connection

In CFS construction, with the aim of loading transfer and support, fasteners can be used to connect individual components such as studs, joists to the primary structure or to each other. Some general types of connection were used in the cold-formed steel construction such as welds, bolts, screws, rivets. The below figures show some types of connection used rivets such as self-piercing rivet, bi and mono component blind rivets and other connection technique, such as adhesive anchors, mechanical anchors, power actuated fasteners (PAF), clinching and structural glue (Figure 2.5).

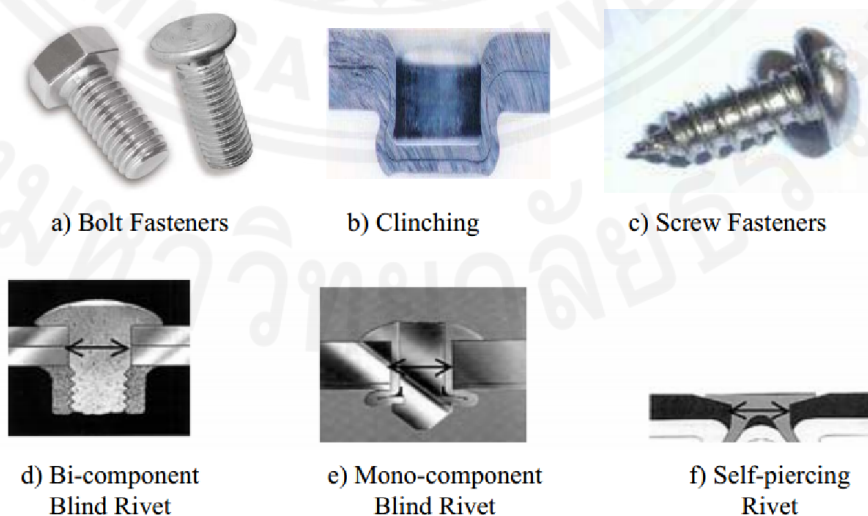


Figure 2.5. Connectors used in CFS construction

Screw is a common type of connections that is used in CFS. Screw connection provides advantages in fast installation and simple design due to the thinness of the CFS. Screwed joints are suitable and effective when applying into the cold-formed steel section with the condition that total thickness should not give difficulty to the self-drilling process. From the above reasons, in this study, the built-up section is connected by using additional stiff plate with 4 screws instead of welding because of its thin thickness and can be increased the ultimate moment capacity of the section to some extent (Figure 2.6). The length of screw is 5cm and the diameter of screw is 1cm.

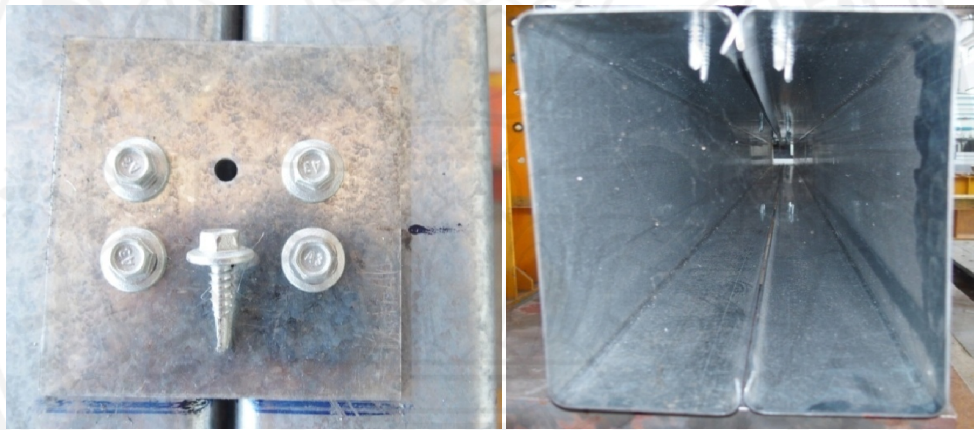


Figure 2.6. Screw connections in the test

## Chapter 3

### Experimental Investigation

#### 3.1. Test specimen

The C-section specimens were supported by BlueScope Lysaght (ThaiLand) Limited Company. GALVSPAN steel was used to produce Cee-section by roll-formed procedure complying with AS1397-1993. All steels used in this test were coated with a zinc alloy. It is assumed that the contribution of metallic coating to the structural strength of LSB in terms of section and member capacities is insignificant and therefore the base metal thickness (BMT) is used instead of the total coated thickness. The BMT of each specimen was determined using the acid itching method. The total coated thickness of each specimen was measured before they were immersed in the hydrochloric acid to wash off the metallic coating. The specimens were taken out after approximately 60 minutes in the hydrochloric acid and were washed in pure water before the BMT was measured. The details of the base metal thickness are listed in Table 3.1.

Table 3.1. Standard range of Cee-section

Section size (mm)	Base metal thickness (mm)
100	1.0, 1.2, 1.5, 1.9
150	1.2, 1.5, 1.9, 2.4
200	1.5, 1.9, 2.4
250	1.9, 2.4
300	2.4, 3.0
350	3.0

These sections are zinc coating of Z275, which are 275 g/m<sup>2</sup> minimum coating mass. There are three sizes of Cee section to assembly the built-up sections which are section standard size of Lysaght cee sections C15019; C15024 and C20019 as the details Table 3.2. Tension tests was applied to define the exact value of material properties of specimens. Span length of the specimen was selected as 4 m based on

current test arrangement capacity. Connector spacings (CS) selected for the specimens are the minimum spacing of span/6, span/4, span/3 and span/2.

Table 3.2. Dimension of C-section use in this research

Specimens	t (mm)	D (mm)	B (mm)	L (mm)	Span (mm)	Connector spacing(mm)
C15019	1.9	152	64	16.5	4000	1750, 1167, 875, 583
C15024	2.4	152	64	18.5	4000	1750, 1167, 875, 583
C20019	1.9	203	76	19.0	4000	1750, 1167, 875, 583

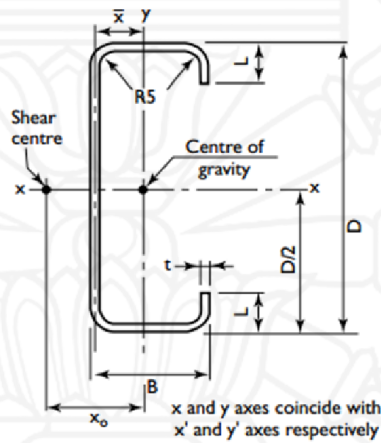


Figure 3.1. C cross section

The built-up sections studied in this research were made from two C-sections with their both flanges placed face-to-face which is connected by using stiffened plates with dimensions of 80x80x1.9mm that were fastened with 4 self-drilling screws (Figure. 3.2). The thickness of C section used for the beams ranges from 1.9 mm to 2.4 mm, flange width of 64 mm and inside corner radius of 5 mm. The lip of C section varies from 16.5 mm to 19.0 mm and the overall depth was 152 mm. As it can also be seen in Fig. 3.2, the built-up section is connected by using stiffened plate with 4 screws instead of welding because of its thin thickness, this will not reduce a capacity of the section.

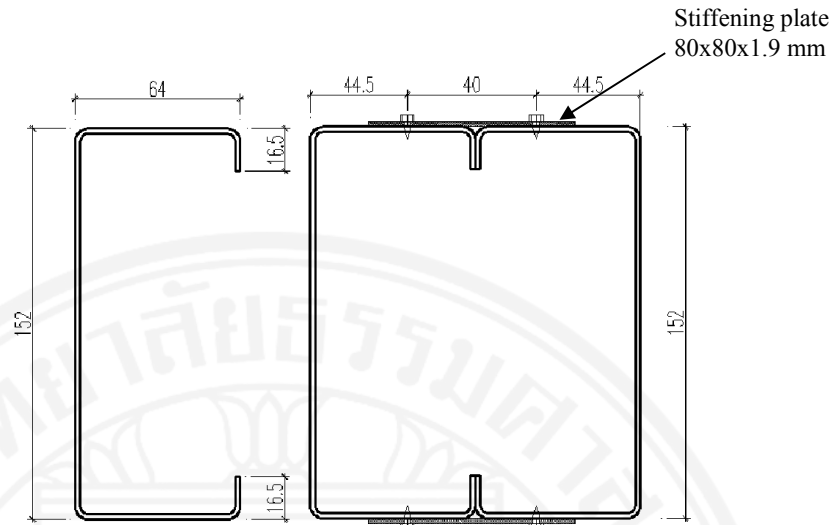
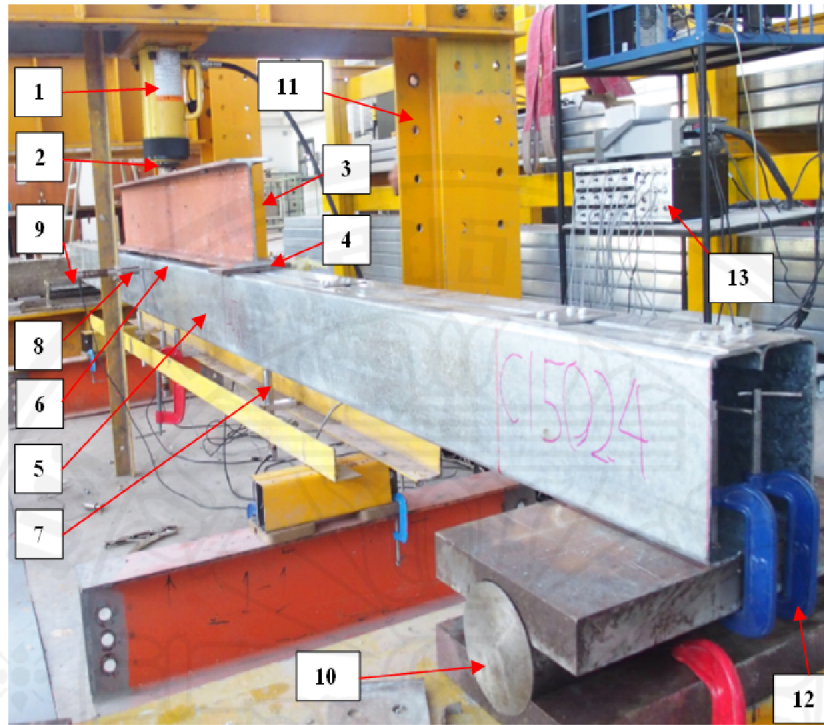


Figure 3.2. Face-to-face built-up C specimen (C15019)

### 3.2. Test set-up

The experimental arrangement of the face-to-face built-up C beams is shown in Figure.3.3. The force was applied at two points by mean of bearing plate (no.4) with length of 10cm that are placed symmetrically to the center of the beam to create a uniform bending moment in the middle span without shear force. In addition, the bearing plate was used in order to distributed the concentrated loading to avoid the localized failure at loading point on the tested beam. The four point bending tests were performed with a MTS Systems machine (Figure. 3.3). During the bending test, a MTS Controller 407 was used to operate the hydraulic jack (no.1). The loads were applied by using manual hydraulic pump connected to hydraulic jack that was hung from steel frame (no.11). To control the applied load during the test, a load cell (no.2) with a measured capacity of 70 kN was positioned beneath the hydraulic jack and connected directly to the monitor. In order to transfer the loading from hydraulic jack to the CFS test beam, the I steel beam (no.3) was used and applied at two bearing plate on the test beam (no.5). A spherical plain bearing with length 20cm was used to make a roller support (no.9) condition which allowed the horizontal displacement but precluded the possible vertical, lateral rotation and also the lateral displacement of the test beams, whereas the other was fixed by clamp (no.12) to prevent the horizontal movement of the beams, namely pinned support (no. 10).





- 1: Hydraulic jack
- 2: Load cell
- 3: I steel beam
- 4: Bearing plate
- 5: Test CFS beam
- 6: Strain gauge
- 7: Vertical LVDT
- 8: Horizontal LVDT
- 9: Roller support
- 10: Pinned support
- 11: Steel frame
- 12: Clamp
- 13 : Data logger

Figure 3.3. Overall view of bending test

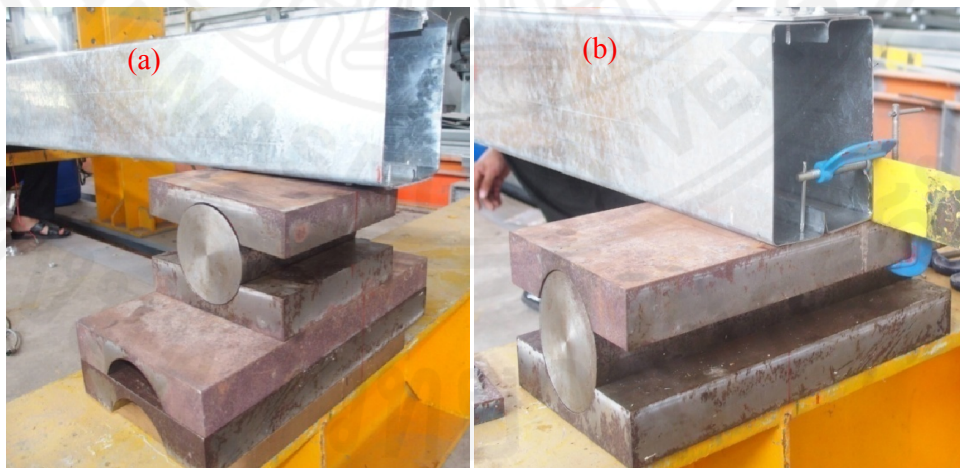


Figure 3.4. Support system: (a): Roller support; (b): Pinned support



Figure 3.5. Detail of measurements : (a):Strain gauge; (b): LVDT;  
(c) (d): data logger

### 3.3. Test procedure

Firstly, a small load was applied on the test beam by using manual hydraulic pump so as to settle equally the loading system. Subsequently, the load was applied gradually until the specimen failed where the recording load was reached the maximum load. To investigate the bending capacity and strength of face-to-face built-up C-sections, the vertical and horizontal deflections as well as strains were measured. The vertical, horizontal displacement was measured using linear variable displacement transducer LVDTs (no.7,8 in Figure. 3.3) of 10cm a maximum displacement capacity. Longitudinal strains were recorded on the top and bottom flange by using 1 cm strain gauges (no. 6 in Figure. 3.3). All data were measured at Section M and recorded by using a TDS-102 data logger (Figure. 3.6).

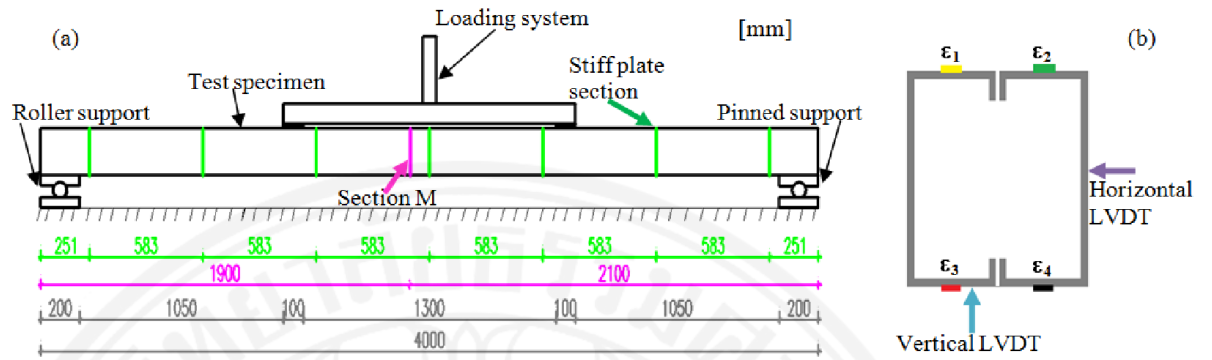


Figure 3.6. (a) Schematic diagram of four-point bending test with CS of L/6; (b) Cross section M

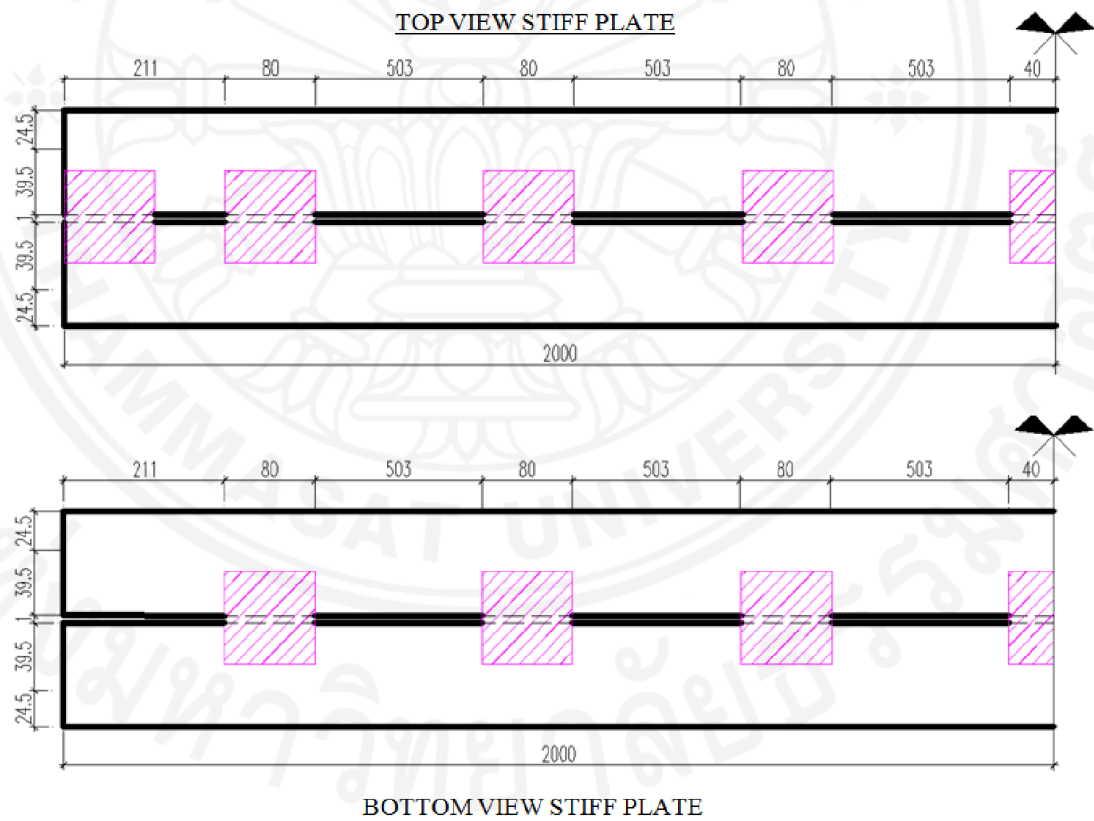


Figure 3.7. Top and bottom view of connector arrangement with CS of L/6

### 3.4. Material properties

The structural behaviour of CFS beams including yield stress, ultimate stress, Young's modulus and stress-strain behaviour depends on the mechanical properties of the steel used. In order to determine the required important mechanical properties, tensile steel coupon tests taken from CFS beams were undertaken based on the procedure specified in the Australian Standard AS1391 (SA, 2007). From various locations of the C-section, namely the flange and web, the tensile steel coupon specimens were taken in the longitudinal direction to conduct the tensile coupon test. It is necessary to design the tensile coupons which limit the possibility of an eccentric connection between the test machine grips and the test coupon. The dimension of all coupon specimens were shown in Figure. 3.8a. There were 2 differences thickness 1.9 mm and 2.4 mm of the material that were used in this research. All the tensile coupons were tested in the Structures Laboratory at the NS Bluescope Steel Thailand Company complying with AS 1391. The measured average stress-strain curves for steel material properties in this research were given in Figure. 3.8b. Tensile steel coupon test results shown that the CFSC-sections used in this study had 485 MPa yield strength ( $F_y$ ) and 528 MPa ultimate strength ( $F_u$ ). In addition, the measured Young's Modulus ( $E$ ) was 200 GPa.

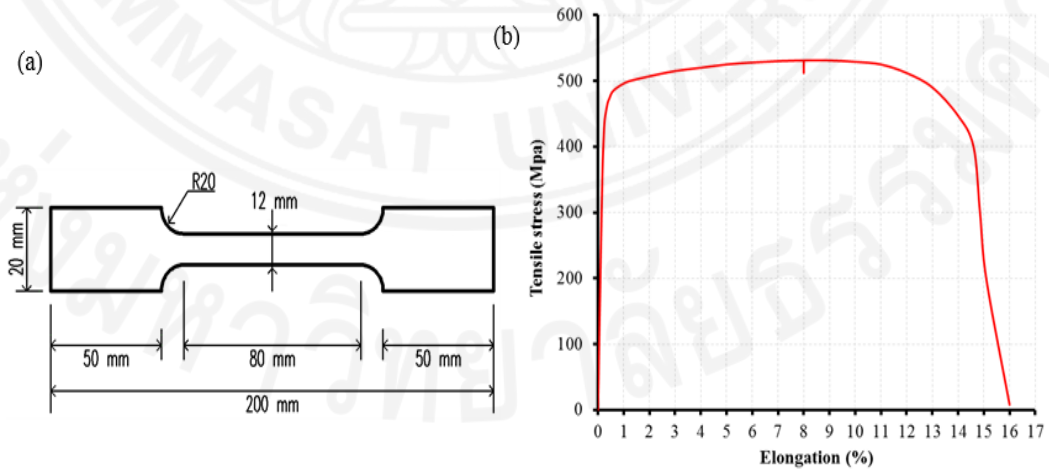


Figure 3.8. (a): Dimension of tensile coupon specimen  
(b): Stress-strain curve for the specimens

### 3.5. Test results

The summary results including maximum load, vertical and horizontal displacement and also the main failure mode of the beam subject to uniform bending test were listed below in Table 3.3.

Table 3.3: Summary test result of the beam corresponding to CS variation

Specimen	Connection spacing d(mm)	Maximum Load(KN)	$\Delta_{VD}$ (cm)	$\delta_{HD}$ (cm)	Main Failure Mode	
					C <sub>1</sub>	C <sub>2</sub>
F2F-C15019	L/6	37.0	4.3	0.5	WB + FB	WB + FB
	L/4	36.5	4.3	0.4	WB + FB	WB + FB
	L/3	34.4	4.0	1.7	WB + FB + LDB	FB + LDB
	L/2	30.5	3.7	1.5	LTB	FDB + LDB
F2F-C15024	L/6	51.5	5.1	0.1	WB + FB	WB + FB
	L/4	48.7	4.9	0.5	WB + FB	WB + FB
	L/3	51.0	5.1	0.1	WB + FB	WB + FB
	L/2	46.5	4.5	1.0	LTB	FDB + LDB
F2F-C20019	L/6	48.0	2.7	0.05	WB + FB	WB + FB
	L/4	47.5	2.6	0.15	WB + FB	WB + FB
	L/3	37.5	2.6	3.30	WB + FB + LDB	FB + LDB
	L/2	36.7	2.5	3.30	LTB	FDB + LDB

\*F2F: face-to-face built-up beam;  $\Delta_{VD}$ : maximum vertical displacement at midspan;  $\delta_{HD}$ : maximum horizontal displacement; L: clear span (3.6m); C<sub>1</sub>: one C section side; C<sub>2</sub>: the other C section side; WB: web buckle; FB: top flange buckle; FDB: flange distortional buckle; LTB: lateral torsional buckle; LDB: lateral distortional buckle; L/6, L/4, L/3, L/2= 583, 875, 1167, 1750mm respectively

As expected, the more connection spacing (CS) increases, the more maximum load decreases to some extent with respect to F2F-C15019, F2F-C15024 and F2F-C20019 section. However, there is a slightly different tendency for F2F-C15024 beam with CS ranging from L/6 to L/3, namely the beam with CS L/4 showed the ultimate load of 48.7kN that is slightly less than the ultimate load of 51 kN for CS L/3. This may be due to the manufacturing CFS section and fabrication the built-up beam process which lead to the material and geometric imperfections in the beam. For this section, there are small variations of maximum load of 51.5, 48.7 and 51 kN between CS L/6, L/4 and L/3, respectively, but slightly insignificant. However, the F2F-C15024 beam with CS of L/2 had the maximum load of 46.5 kN that is 10% less than the one of spacing L/6. For F2F-C15019 beam, it is observed that the beam with the CS of L/6 and L/4 had the ultimate load of 37 and 36.5 kN, respectively, that is the highest load compared with the other beams with CS of L/3 and L/2. In

contrast, the F2F–C15019 beam with the maximum CS of L/2 had the minimum ultimate load of 30.5kN only that is 18% less than the one of spacing L/6. Also found from Table 3.3 is that the difference of ultimate load between beam with CS L/6 and L/4 is insignificant. The same tendency was also observed for F2F–C20019 beam. The insignificant difference of ultimate load between beam with CS L/6 and L/4 is observed. The beam with CS of L/6 and L/4 had the ultimate load of 48 and 47.5 kN, respectively, that is the highest load compared with the other beams with CS of L/3 and L/2. The beam with CS of L/2 had the minimum ultimate load of 36.7kN only that is 24% less than the one of spacing L/6. As an experimental result, it can be concluded that the CS affected significantly the maximum load. Reducing the connection spacing from L/2 to L/6 can increase about 10%-24% ultimate load of the beam.

For F2F–C15019 beam, it can be seen that the horizontal displacement (HD) of with CS L/3 and L/2 is much higher than that of the beam with CS L/6 and L/4 (Figure.3.9). The curve revealed that the HD for CS L/6 and L/4 exhibited only a small displacement from the beginning until the beam reach the maximum load at a small value of 5mm, which mean that the main failure mode is pure local buckling while the HD for CS L/3 and L/2 occurred rapidly at about 80% or more of maximum load and exhibited larger value of 17mm at the ultimate load. This was due to the premature lateral rotation governing the buckling behavior and displacement of the beam. On the other hand, the curve change sharply at its peak when beam reach ultimate load, which means that the beam failed suddenly with respect to CS L/6 and L/4, whereas for CS L/3 and L/2 the gradual failure occurred near the ultimate load. The reason for this phenomenon of CS L/3 and L/2 was the small global lateral-torsional buckling occurring at the beginning of the loading governing buckling failure mode. Figure. 3.15 shown that the main failure mode for F2F–C15019 beam with CS L/3 and L/2 is interactive buckling mode and the main failure mode for CS L/6 and L/4 is local buckling including web buckling and flange buckling. Similar behavior obtained for F2F–C20019 beam from Figure. 3.15 shown that the local buckling is the main failure mode for F2F–C20019 beam with CS L/6 and L/4, whereas the complex buckling mode including web, top flange, lateral

torsional, flange distortional buckling interaction is the main failure mode for F2F–C20019 beam with CS L/3 and L/2. For F2F–C15024 beam, the phenomena for failure mode observed with respect to CS L/6, L/4 and L/2 were similar to that of F2F–C15019 and F2F–C20019 beam with the same CS, except L/3 which the main failure mode was local buckling (Figure.3.15). From Table 2, there are inconsiderable differences of vertical deflection between F2F–C15024 beam with CS of L/6, L/4 and L/3 varying from 5.1; 5.0 and 5.1, respectively. The same trend was also found in Table 3.3 for horizontal displacement of F2F–C15024 beam with CS of L/6, L/4 and L/3.

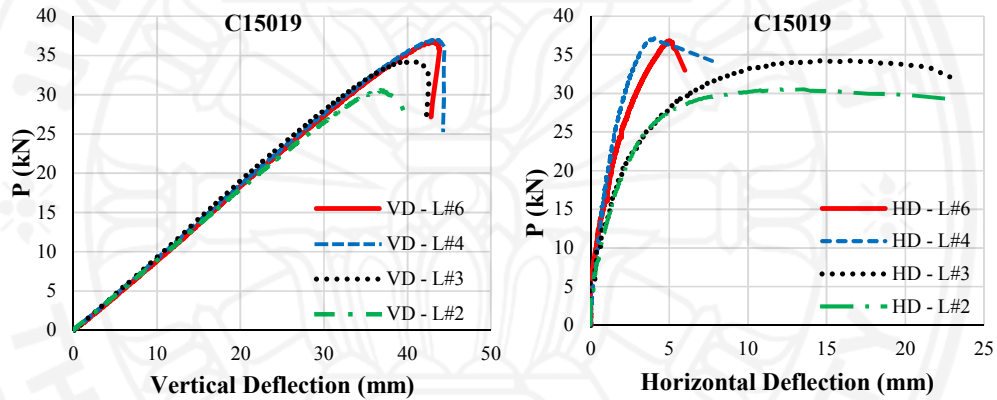


Figure 3.9. : Load-displacement curve for F2F–C15019 with CS L/6; L/4; L/3; L/2

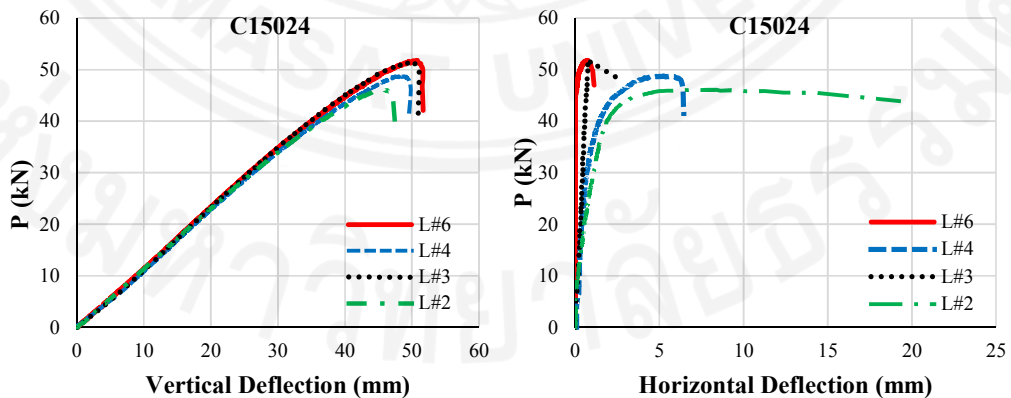


Figure 3.10.: Load-displacement curve for F2F–C15024 with CS L/6 ; L/4; L/3; L/2

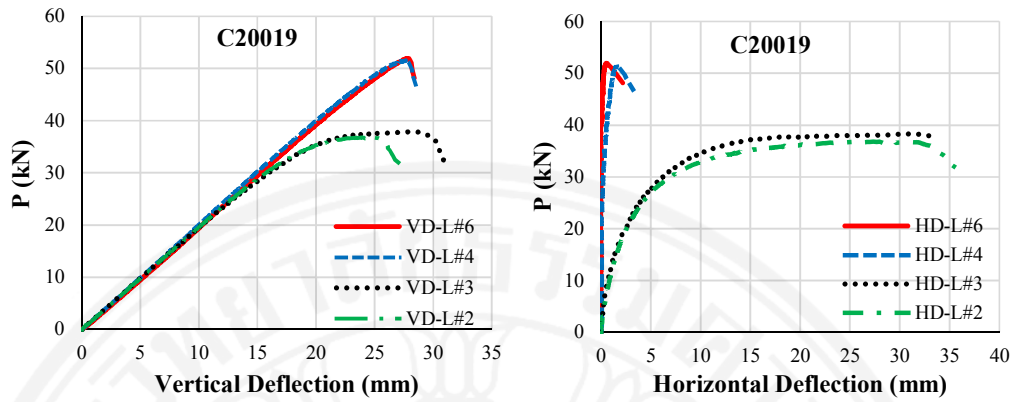


Figure 3.11: Load-displacement curve for F2F-C20019 with CS L/6;L/4;L/3; L/2

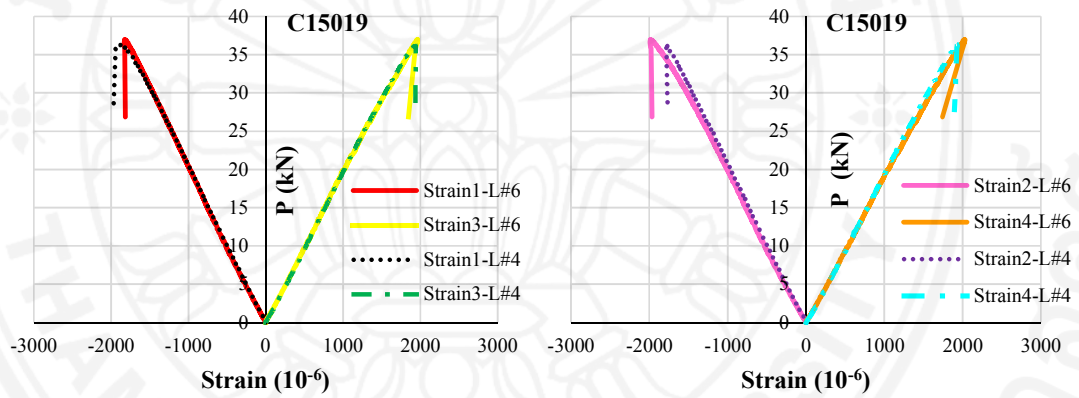


Figure 3.12. : Load-strain for F2F-C15019 with CS of L/6, L/4

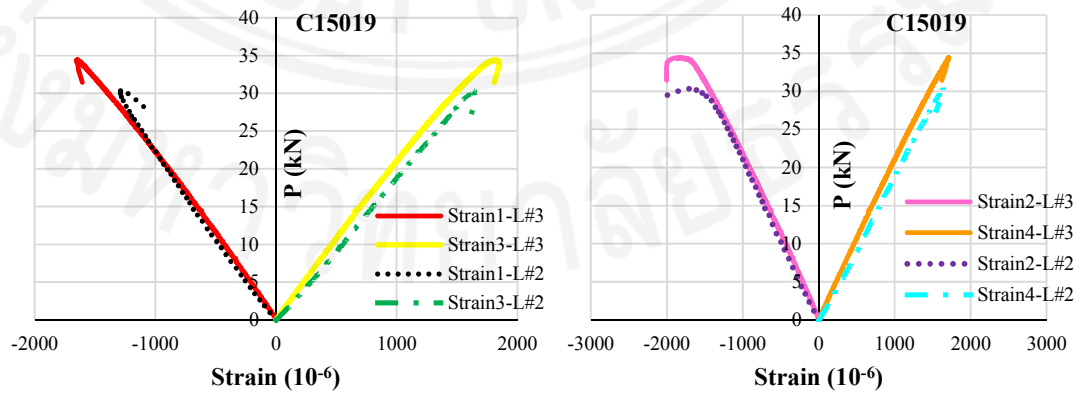


Figure 3.13.: Load-strain for F2F-C15019 with CS of L/3, L/2



The evolution of longitudinal strain ( $\epsilon$ ) versus load was showed in Figure. 3.12-3.13 at midspan section. For all beams, the similar tendency of all strain gauges ( $\epsilon_3, \epsilon_4$ ) positioned at bottom flange (tensile flange) was observed during the loading. Some connection spacings, such as  $L/3$  and  $L/2$ , when the load reached around 80% loading capacity, the difference between strain gauges ( $\epsilon_1, \epsilon_2$ ) evolution at top flange (compressive flange) was observed until the ultimate capacity. The reason for this phenomenon may be due to lateral rotation occurring at about 80% or more of maximum load that induced twisting behavior and separated two compressive flange part such as different level between two top flange (Figure. 3.13).

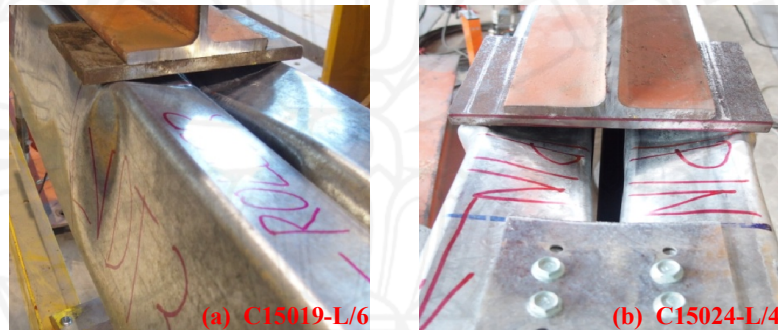


Figure 3.14. Local buckling for: (a) C15019 with CS  $L/6$  ;  
(b) C15024 with CS of  $L/4$

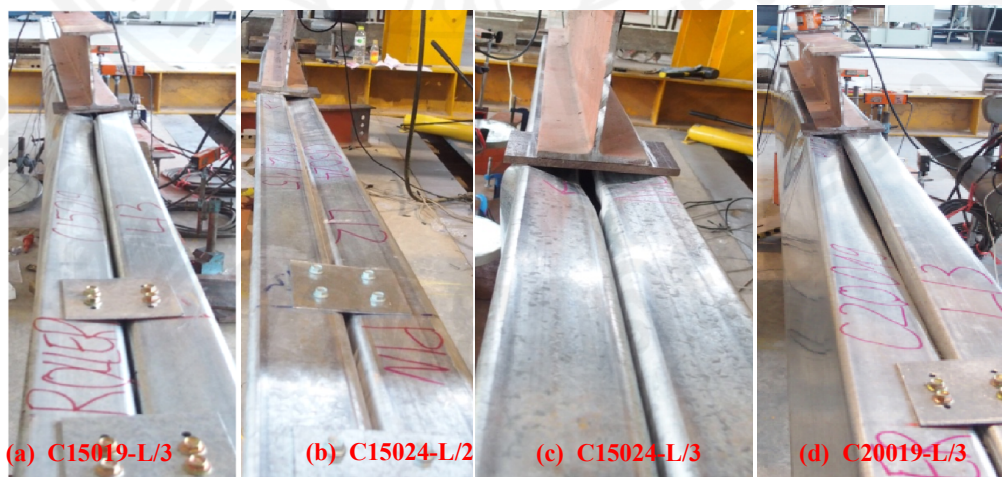


Figure 3.15. Failure mode for: (a) C15019 with CS of  $L/3$ ; (b)(c) C15024 with CS of  $L/2$  and  $L/3$ ; (d) C20019 with CS of  $L/3$

Table 3.4 shows the summary results including ultimate load ( $P_u$ ) and flexural moment capacity of the test ( $M_t$ ) for 12 built-up beams. Other values such as yield moment ( $M_y$ ), the critical elastic lateral-torsional buckling moment of the section ( $M_{cre}$ ), the critical elastic local buckling moment of the section ( $M_{crl}$ ), the critical elastic distortional buckling moment of the section ( $M_{crd}$ ) as calculated by using the computer software CUFSM were also listed below in Table 5.1. It is apparent that the nominal moment capacity obtained from a design rule ( $M_n$ ) with continuous connection was close to the moment capacity obtained from the tests ( $M_t$ ) with respect to the minimum connection spacing ( $L/6$  and  $L/4$ ) for all sections and  $L/3$  for section F2F-C15024 which was failed by local buckling (web buckling + top flange buckling). The good agreement of moment capacity between the test and design rule proves that the conservative of the Specification for the face-to-face CFS built-up beam that was governed by local buckling at failure mode.

Table 3.4: Comparison of moment capacity from test and design rule for built-up face-to-face C-section beam

Specimen	Test results		Design results	Test/Design
	d (mm)	$M_t$ (kNm)	$M_n$ (kNm)	$\frac{M_t}{M_n}$
F2F-C15019	L/6	21.28	20.4	1.04
	L/4	20.90		1.03
	L/3	19.78		0.97
	L/2	17.54		0.85
F2F-C15024	L/6	29.61	28.78	1.02
	L/4	28.00		0.97
	L/3	29.32		1.02
	L/2	26.74		0.92
F2F-C20019	L/6	27.60	27.47	1.00
	L/4	27.31		0.99
	L/3	21.56		0.78
	L/2	21.10		0.76

\*F2F: face-to-face built-up beam; d: connection spacing.

## **Chapter 4**

### **Numerical Investigation**

#### **4.1. Introduction**

After experimental investigation, a numerical model was developed using ABAQUS (version 6.12) to compare with the test results. At present, since computing machines and finite element programs have been improved endlessly, this provides a moderately time-consuming and inexpensive alternative to experimental method. The finiteelement analysis (FEA) is therefore the most efficiently computational tool to perform the investigation into the behaviour and ultimate member capacities of CFS built-up section under flexural loading condition. The effects of nonlinear material, imperfections of geometry, contact behavior, application of load and the boundary conditions should be included to represent the actual member so as to get the accuracy of the results on the numerical model close to reality.

For this purpose, the finite element models of face-to-face CFS built-up C section was developed. This section describes the details of the development of numerical model of CFS built-up section. The experimental models including the effects of material and geometric non-linearities, initial geometric imperfections and contact behaviour were developed and compared with the test results. The CFS beam subjected uniform bending moment was simulated by ABAQUS v6.12 (Figure 4.1).

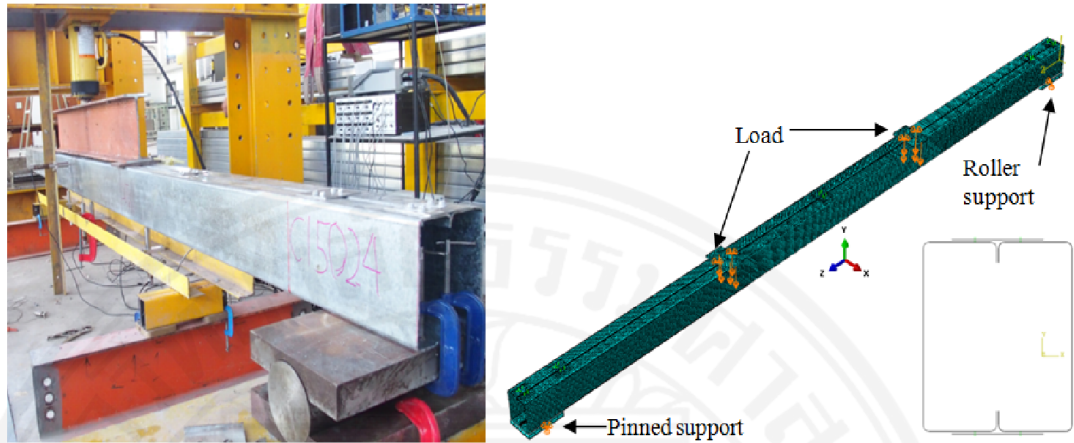


Figure 4.1. FEM model for beam with connection spacing  $L/2$

#### 4.2. Finite element and mesh

The thickness of CFS sections ranges from 1.9 to 2.4 mm, which is comparatively less than the other two dimensions. Thick element formulation is based on Mindlin/Reissner theory, which does account for transversing shear deformation, whereas thin element formulation is based on Kirchhoff theory, which neglects transverse shear deformation. Shell elements (S4R) was used to model CFS beam and the stiff plate, whereas the bearing plate and support were modeled by using solid elements (C3D8R). The shell elements (S4R) was selected because it is suitable for both thin and thick element for CFS sections. This type of element in ABAQUS uses second-order reduced integration. Reduced integration usually provides significant reduction in computing time and more accurate result, especially in three dimensions. It is also isoperimetric quadrilateral shell element including four node. Each node has six degrees of freedom. Moreover in this area, this type of element (S4R) was often used by many researchers in their numerical analyses. There was no screw failures observation during the tests. Therefore, to simplify screws, fasteners function was used to model to screw by constraining all rotational and translational degrees of freedom of the nodes at the screw location. Convergence studies were carried out to evaluate the effect of element size on the result. It was found that the element size of  $10 \times 10\text{mm}$  for C section is appropriate to obtain the good result.

Fine meshes was generated at the inside corner radius of C section to achieve the stress concentration (Figure 4.2).

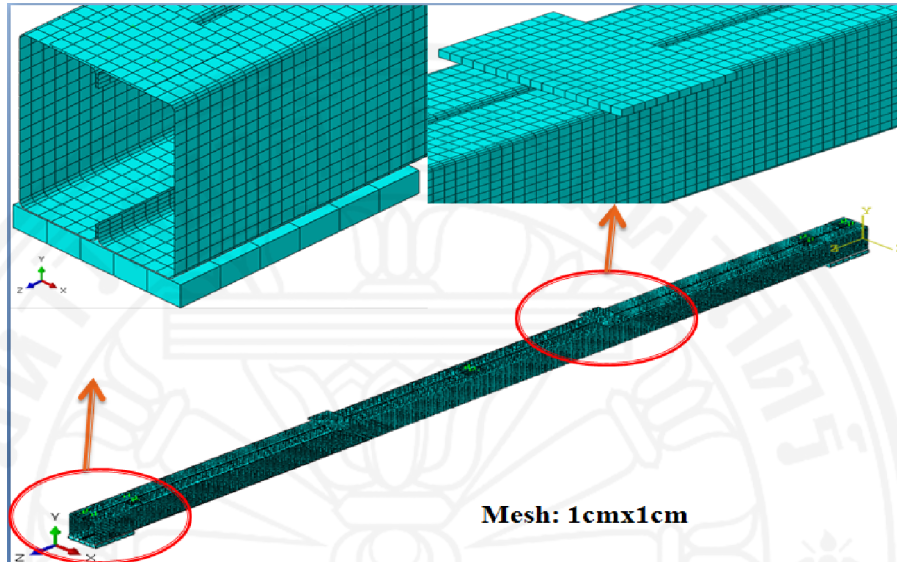


Figure 4.2. Mesh modelling

#### 4.3. Material modelling

The Material non-linearity used in this numerical analysis for CFS was based on the tensile coupon tests reported by Lysaght-Blue Scope company. The sections used in the test had 485 MPa yield strength ( $F_y$ ) and 528 MPa ultimate strength ( $F_u$ ). The Young's Modulus of 200 GPa was also obtained from the tensile coupon test. During the tests, there was no stiff plate failures observation. Therefore, an elastic stress-strain was used to simulate the steel stiff plate with the assumed properties of Young's Modulus ( $E$ ) = 200 GPa and the Poisson's ratio = 0.3. A rigid bearing plate and support were modelled as rigid solid element with high Young's Modulus. Cold-work due to forming and residual stresses were ignored.

#### 4.4. Loading, boundary and contact condition

To simulate the loading on the beam, the controlled displacement was imposed vertically with Y direction on the bearing plate. There are additional restraints in X

and Z-direction located at the middle of the plate to prevent the lateral and longitudinal movement of the plate as it can be seen in the experiment (Figure 4.4a). The supported boundary conditions implemented in the three dimensional numerical model are generated with great accuracy. To model the pinned support, all translations of the nodes located at the middle bottom surface were constrained, i.e., about X, Y and Z-axis, whereas the roller support only the translations in the directions X and Y were constrained (Figure 4.4b, c).

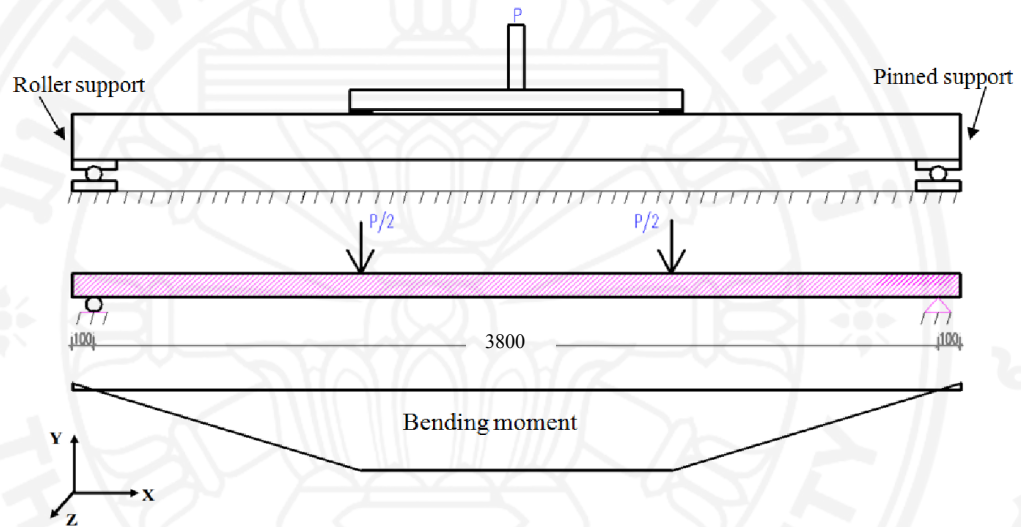


Figure 4.3. A simplified model for four-point bending test

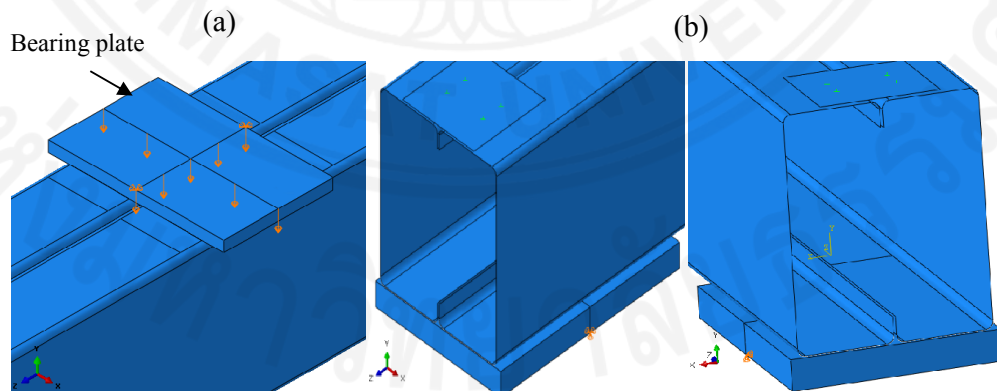


Figure 4.4. (a) Loading modelling, (b) A simplified pinned,roller support conditions

A tie contact modelling was applied in order to simulate the interaction between the rigid support and the bottom surface of C section as seen in Figure 4.5. There are also contact between the two lip of C section together and between the top flange and the rigid bearing plate(Figure 4.6). A surface-to-surface contact with finite sliding, frictionless, “hard” contact pressure-overclosure properties was used to represent the interaction between them. For contact between the two lip of C section, contact surface of one lip C section was assigned as master surface while contact surface of other lip C section was assigned as slave-surface (Figure 4.7).

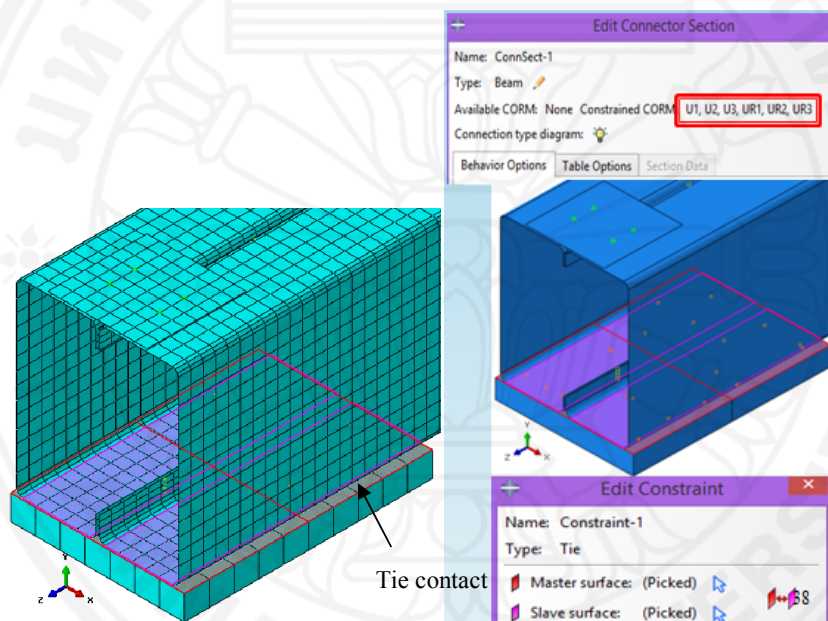


Figure 4.5. Contact modelling between the rigid support and C section

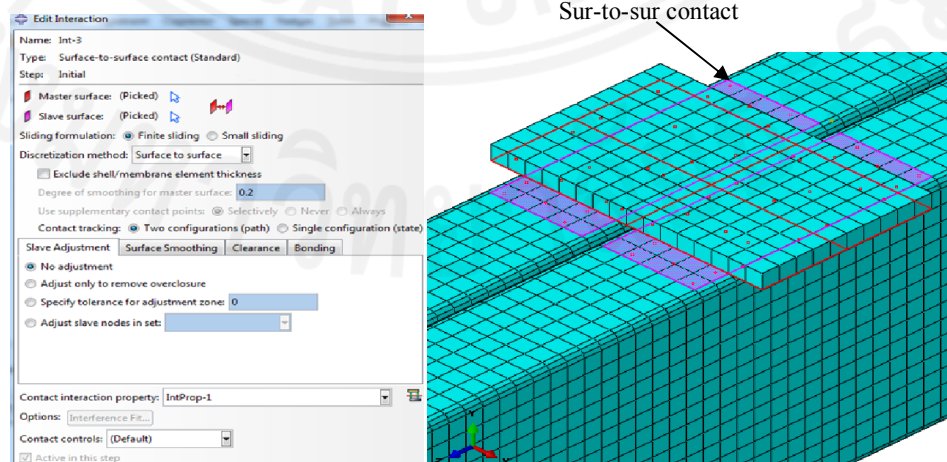


Figure 4.6. Contact modelling between the rigid bearing plate and C section

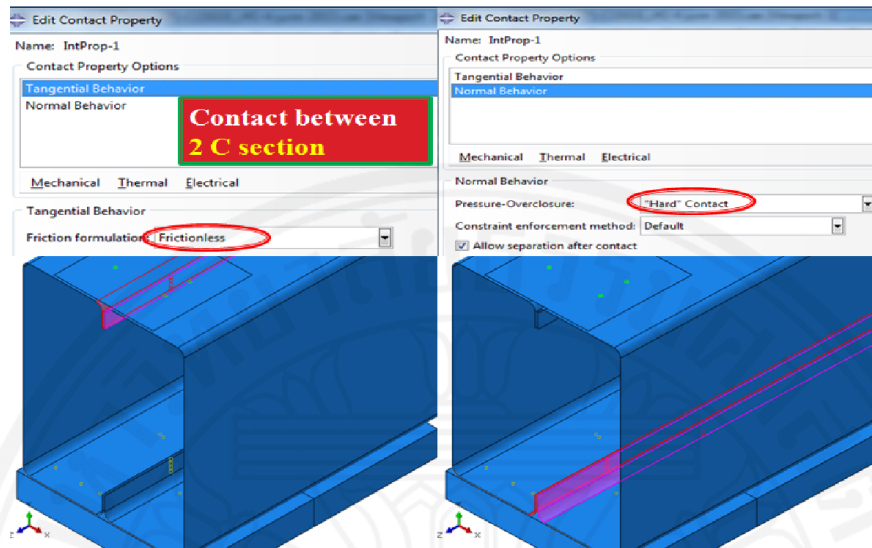


Figure 4.7. Contact modelling between two lip of C section

#### 4.5. Finite element analysis

The finite element models (FEM) of face-to-face CFS built-up C section was developed including the effects of material nonlinearities, initial geometric imperfections. A geometric imperfection plays a crucial role to the flexural behaviour of thin-walled structures, especially at the maximum load stage. Therefore, a linear buckling analysis was first implemented without imperfections to obtain the buckling mode shape which represents the failure shape of structure corresponding to each mode. After that, the first buckling mode shape obtained from a linear buckling analysis was scaled by a factor to establish a geometric imperfection in the model. Finally, the nonlinear analysis including geometric imperfection was performed to simulate the flexural behaviour of CFS beam.

#### 4.6. Comparison between numerical and test results

##### 4.6.1 Load–vertical displacement comparison

The ultimate load and main failure mode of CFS beam obtained from numerical analysis were compared with test results as summarized in Table 4.1. It was observed that the ultimate load obtained from



numerical analysis is in good agreement with the test results. From Table 4.1, there are inconsiderable differences of the FEM-to-test ultimate loading capacity ratio varying from 0.94 to 1.01 for all beams. The load–vertical displacement curves at midspan of beam were also presented and compared with test results in Figure 4.8. The FEM curves agree well with the test curves from beginning to maximum loading stage.

Table 4.1 Comparison of FEM and test results

Specimen	d (mm)	Experiment results			$P_{FEM}$ (KN)	FEM results		$\frac{P_{FEM}}{P_{max}}$	
		$P_{max}$ (KN)	Main failure mode			$P_{max}$	Main failure mode		
			$C_1$	$C_2$			$C_1$		$C_2$
F2F-C15019	583	37.0	WB + FB	WB + FB	35.1	WB + FB	WB + FB	0.95	
	875	36.5	WB + FB	WB + FB	34.2	WB + FB	WB + FB	0.94	
	1167	34.4	WB + FB + LDB	FB + LDB	34.0	WB + FB + LDB	FB + LDB	0.99	
	1750	30.5	LTB	FDB + LDB	30.2	LTB	FDB + LDB	0.99	
F2F-C15024	583	51.5	WB + FB	WB + FB	50.2	WB + FB	WB + FB	0.98	
	875	48.7	WB + FB	WB + FB	49.6	WB + FB	LTB + FB	1.01	
	1167	51.0	WB + FB	WB + FB	50.4	WB + LTB	FDB + LDB	0.99	
	1750	46.5	LTB	FDB + LDB	46.1	LTB	FDB + LDB	0.99	
F2F-C20019	583	48.7	WB + FB	WB + FB	41.1	WB + FB	WB + FB	1.11	
	875	47.5	WB + FB	WB + FB	44.5	WB + FB	WB + FB	1.18	
	1167	37.5	WB + FB + LDB	FB + LDB	47.0	WB + FB + LDB	FB + LDB	0.91	
	1750	36.7	LTB	FDB + LDB	47.6	LTB	FDB + LDB	0.91	

\*F2F: face-to-face built-up beam; d: connection spacing;  $C_1$ : one C section side;  $C_2$ : the other C section side; WB: web buckle; FB: top flange buckle; FDB: flange distortional buckle; LTB: lateral torsional buckle; LDB: lateral distortional buckle; L/6, L/4, L/3, L/2= 583, 875, 1167, 1750mm respectively.

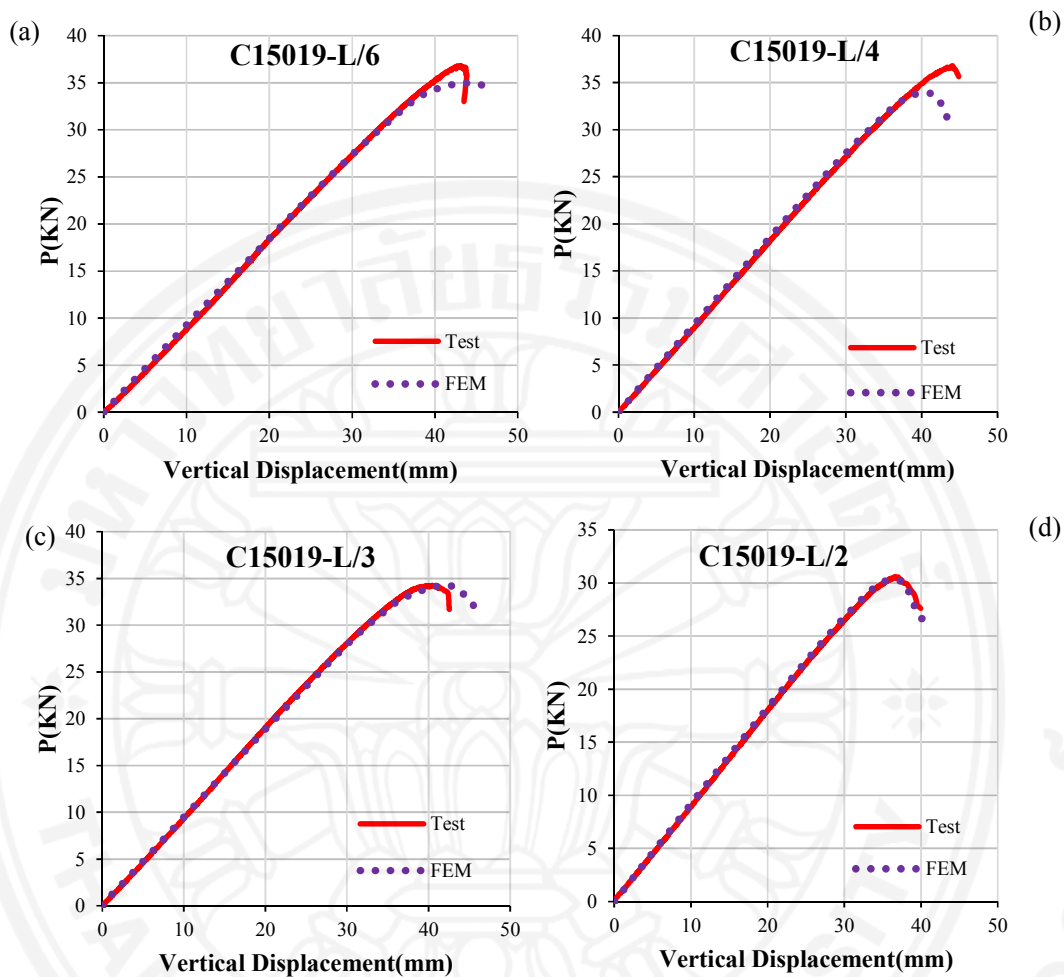


Figure 4.8. Load-vertical displacement comparison between FEM and test results for C15019 beam with different connector spacing:  
(a) 583mm; (b):875mm; (c):1167mm; (d):1750mm

#### 4.6.2. Main failure mode

All buckling modes of CFS structure such as web buckling, top flange buckling, flange distortional buckling, lateral torsional buckling, lateral distortional buckling and their interaction were observed in FEM results. The details of FEM failure modes are presented in Table 4.1. The comparison of failure modes of C15019 beam between FEM and test are also shown in Figure 4.9. Most of failure modes obtained from FEM

are in good agreement with the test results, but are not identical for C15024 beam with connector spacing  $L/3$ .

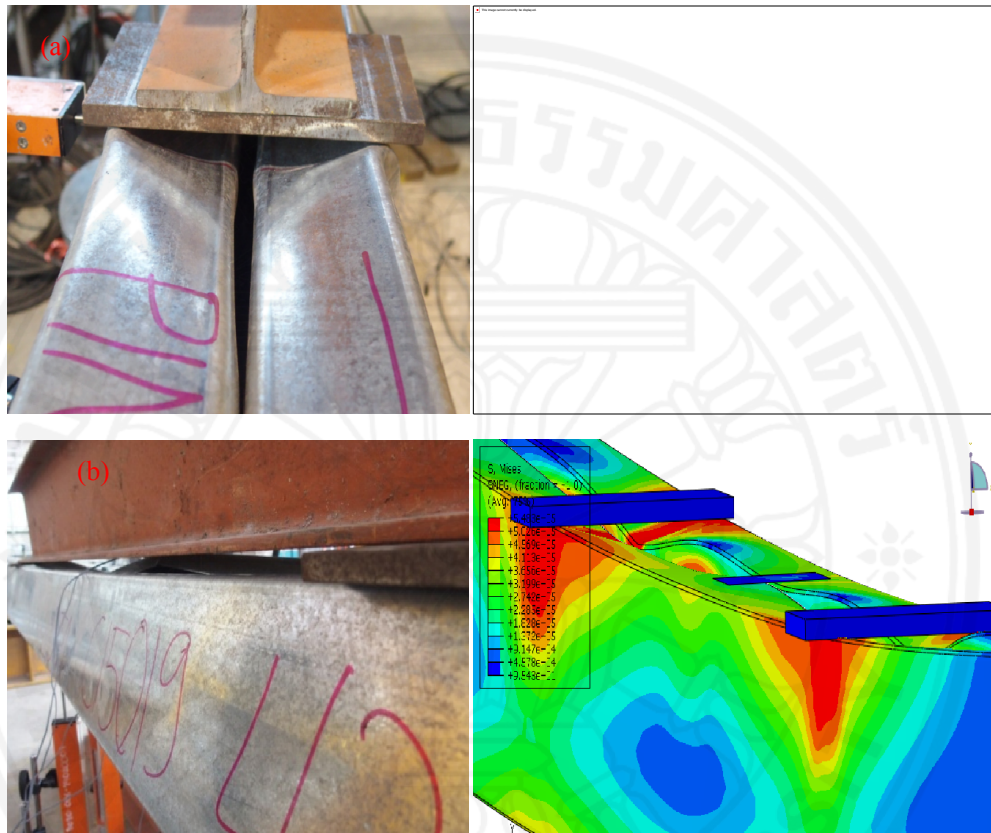


Figure 4.9: Main failure mode comparison between test and FEM test results for C15019 beam with different connector spacing: (a):583mm; (b):1750mm

## Chapter 5

### Conclusions and Recommendation

The details of a experimental and numerical analyses were presented in this paper with the purpose of investigating the buckling behaviour of face-to-face C-section beam. Firstly, a series of pure bending tests was undertaken and presented in this study by using three CFS section C15019, C15024 and C20019. The test results showed that for the C15019 and C20019 beam, the maximum load and failure mode are the same for the case of  $L/6$  and  $L/4$ . Similar conclusion was also drawn for the C20019 beam, the maximum load and failure mode are the same for the case of  $L/6$  and  $L/4$ . For the C15024 beam, the maximum load and failure mode are the same for the case of  $L/6$ ,  $L/4$  and  $L/3$ . This means that limit connection spacing of  $L/6$  stipulated in AISI-2012 may be unconservative.

A nonlinear finite element analysis was generated to simulate the test beam. The results from numerical analyses were compared with the test results to validate the model. Good agreement was obtained between experimental and numerical results, proving the validity of the proposed FEM in this study.

To evaluate the beam strength from tested results, a comparison between the experimental results and design strength given by the available design equations specified in North American Specification AISI (2012 ed.) was then performed. The good agreement of moment capacity between the test and design rule proves that the conservative of the Specification for the face-to-face CFS built-up beam that was governed by local buckling at failure mode.

For future research, parametric studies are recommended using the above finite element model (FEM) in order to investigate the influence of the thickness, height, beam's length and connection spacing of the beams on its buckling behaviour. Based on the results from the parametric studies, a simple equation is developed to calculate the ultimate moment capacities of CFS face-to-face C-section beam failing mainly by global buckling without conducting all full-scale tests that is inevitably very time-consuming and expensive.

## References

- AISI, Cold-formed steel framing design guide, American Iron and Steel stiffeners ,  
*Journal of Institute*. 1st ed., 2002, 2nd ed., 2007.
- AS/NZS. Australian/New Zealand standard–cold-formed steel structures, AS/NZS  
4600:2005. 2005, Standards Australia/Standards New Zealand, Sydney.
- ABAQUS/CAE. Version 6.12, USA.(www.simulia.com);2010 .
- Di Lorenzo, G., Portioli, F. and Landolfo R. (2006), Experimental Investigation on  
the Load Bearing Capacity of Built-up Cold-Formed Steel Beams,  
*Proceeding of the International Colloquium on Stability and Ductility  
of Steel Structures*, Lisbon, Portugal.
- C.H. Pham, G.J. Hancock., “Experimental investigation and direct strength design of  
high-strength, complex C-sections in pure bending”, *J. Struct. Eng.* 139  
(11) (2013), 1842–1852.
- EC3, Design of steel structures–Part 1–3: General rules–supplementary rules for  
cold-formed members and sheeting, EN1993-1-3, European Committee  
for Standardization, Brussels, 2006.
- Haiming Wang and Yaochun Zhang (2009) “Experimental and numerical  
investigation on cold-formed steel C-section flexural members”. *Journal  
of Constructional Steel Research*, 65,1225-1235.
- Hancock, G. J., T. M. Murray, and D. S. Ellifritt: Cold-Formed Steel Structures to  
the AISI Specification, Marcel Dekker, New York, 2001
- Iman Faridmehr, M.Md. Tahir, M.H. Osman, A.F Nejad, Reza Hodjati., “An  
experimental investigation of stiffed cold-formed C-channels in pure  
bending and primarily shear conditions”, *Thin-Walled Structures*, 96  
(2015) 39-48.

- Lei Xu, Papiia Sultana, Xuhong Zhou (2009) "Flexural strength of cold-formed steel built-up box sections". *Thin-Walled Structures*, 47, 807-815.
- LuísLaím, João Paulo C. Rodrigues, Luis Simões da Silva (2013)" Experimental and numerical analysis on the structural behavior of cold-formed steel beams". *Thin-Walled Structures*,72,1-13.
- Lennon, R., Pedreschi, R. and Sinha, B.P. (1999). "Comparative Study of Some Mechanical Connections in Cold-formed Steel", *Construction and Building Materials*, Vol. 13, No. 3, pp. 109-116.
- N.T. Nguyen, T.C. Fung, B. Young, "Strength and behavior of cold-formed steel Z-sections subjected to major axis bending", *J. Struct. Eng.* 132 (10) (2006), 1632–1640.
- Nowak, A. S., ASCE, A. M. and Regupathy, P. V. (1984), "Reliability of Spot Welds in Cold-Formed Channels", *Journal of Structural Engineering*, Vol. 110, pp. 1265-1277.
- Schafer. BW. CUFSM: elastic buckling analysis of thin-walled members by finite strip analysis. CUFSM. Version 4.05.<http://www.ce.jhu.edu/bschafer/cufsm/>. Visited on 14 Nov 2015.
- Serrette, R.L., " Performance of Edge-Loaded Cold Formed Steel Built-up Box Beams", *Practice Periodical on Structural Design and Construction*, ASCE, Vol.9, No. 3, 2004,pp. 170-174.
- Xuhong Zhou,Yu Shi.(2011) "Flexural Strength Evaluation for Cold-Formed Steel Lip-Reinforced Built-Up I-Beams".*Advances in Structural Engineering*. Vol.14, No. 4.
- Yu. WW, Roger. A. L. Cold-formed steel design. 4th ed. New York: Wiley; 2010.
- Yu. C, Schafer. BW, "Local buckling tests on cold-formed steel beams", *J. Struct. Eng.* 129 (12) (2003), 1596–1606
- Yu. C, Schafer. BW, "Distortional buckling tests on cold-formed steel beams", *J. Struct. Eng.* 132 (4) (2006), 515–528